Int J Earth Sci (Geol Rundsch) (2017) 106:549–567
DOI 10.1007/s00531-016-1409-x

ORIGINAL PAPER

Late Variscan deformation in the Iberian Peninsula; a late feature in the Laurentia–Gondwana dextral collision

R. Dias[1,2,3] · **N. Moreira**[1,3] · **A. Ribeiro**[4] · **C. Basile**[3]

Received: 5 February 2016 / Accepted: 5 October 2016 / Published online: 27 October 2016

Abstract The Late Variscan deformation event in Iberia is characterized by an intraplate deformation regime induced by the dextral oblique collision between Laurentia and Gondwana. This episode in Iberia is characterized by NNE–SSW brittle to brittle–ductile strike-slip faults, which are considered by the classic works as sinistral strike-slip faults. However, the absence of Mesozoic formations constraining the age of this sinistral kinematics led some authors to consider it as the result of Alpine reworking. Structural studies in Almograve and Ponta Ruiva sectors (SW Portugal) show that NNE–SSW faults have a sinistral kinematics and are occasionally associated with E–W dextral shears. Moreover, this kinematics is related to the late deformation episodes of Variscan orogeny. In Almograve sector, the Late Variscan structures are characterized by NNE–SSW sinistral kink bands, spatially associated with E–W dextral faults. These structures are contemporaneous and affect the previously deformed Carboniferous units. The Ponta Ruiva Sector constrains the age of deformation because the E–W dextral shears affect the Late Carboniferous (late Moscovian) units, but not the overlying Triassic series. The new data show that the NNE–SSW and the E–W faults are dynamically associated and result from the Late Variscan deformation episode. The NNE–SSW sinistral faults could be considered as second-order domino structures related to first-order E–W dextral shears, linked to Laurentia–Gondwana collision during Late Carboniferous–Permian times.

Keywords Iberia Variscan orogeny · Late Variscan deformation · South Portuguese Zone · Kink bands

✉ N. Moreira
nmoreira@estremoz.cienciaviva.pt

[1] Earth Sciences Institute (ICT), Pole of the University of Évora, Rua Romão Ramalho, n° 59, 7000-671 Évora, Portugal

[2] Dep. Geociências da Escola de Ciências e Tecnologia da Universidade de Évora (ECTUE), Largo dos Colegiais, 2-Apartado 94, 7002-554 Évora, Portugal

[3] Laboratório de Investigação de Rochas Industriais e Ornamentais da ECTUE, Convento das Maltezas, 7100-513 Estremoz, Portugal

[4] Centro de Geologia da Universidade de Lisboa (UL), Dep. Geologia da Faculdade de Ciências da UL, Museu Nacional de História Natural e da Ciência (UL), Edifício C6, Piso 4, Campo Grande, 1749-016 Lisbon, Portugal

Introduction

A complex network of major shear zones was developed during the last stages of intracontinental deformation of the Variscan orogeny. This Late Variscan deformation episode was considered the result of internal deformation along first-order E–W dextral shear zones (Arthaud and Matte 1975, 1977). Such kinematics is often considered a pervasive feature of most of the Variscan orogenic evolution (Ribeiro et al. 1995; Shelley and Bossière 2000, 2002; Ribeiro 2002; Ribeiro et al. 2007; Martínez Catalán 2011; Nance et al. 2012; Dias et al. 2016). In the Iberian Massif, this Late Variscan deformation gave rise to some of the most important observed basement faults (Ribeiro 1974; Iglesias and Ribeiro 1981), like the NNE–SSW Vilariça and Régua-Chaves-Verin faults in NW Iberia (Ribeiro et al. 1990; Marques et al. 2002; Moreira et al. 2010; Dias et al. 2013). Although several works focus on this major event, there are still some doubts concerning the kinematics and the timing of the deformation. Such controversy mainly results from the strong reworking of the Late Variscan

structures by the Meso-Cenozoic deformation episodes. The scarcity of Lower Mesozoic outcrops in the vicinity of these major structures strongly limits the temporal constrain of observed deformations to the Palaeozoic. The transition between the Late Variscan wrench faulting and the early Alpine extensional regime is essential to the understanding of the Late Palaeozoic dynamics of Western Europe. In such a debate, the Variscan kinematics of the NNE–SSW main faults is crucial because they have been considered, either sinistral (Ribeiro 1974; Ribeiro et al. 2007; Moreira et al. 2010, 2014; Dias and Basile 2013), or dextral with a sinistral kinematics alpine reworking (Marques et al. 2002). Obviously such opposite interpretations give rise to strongly different geodynamical models for the transition between the late stages of the collision that formed the Pangaea and the beginning of its dispersion leading to the opening of the Atlantic Ocean.

The SW Portuguese coast, where the outcrops are remarkably well exposed, is a key sector to discriminate between the previous models. Indeed, in this region it is possible to highlight:

- A continuity between the sedimentation of the Upper Carboniferous turbiditic sediments (Moscovian; Pereira et al. 2007) and the late stages of the Variscan deformation (Dias and Basile 2013);
- The influence of the brittle–ductile Late Variscan structures in the opening of the intracontinental Triassic rift basins (Dias and Ribeiro 2002; Dias and Basile 2013).

In this paper, new detailed structural mapping in two key sectors of SW Portugal enables the understanding of the kinematical, chronological and geodynamical behaviour of the Late Variscan deformation in Iberia.

Geological setting of Southwest Iberian Variscides

The main Variscan structure in the South Portuguese Zone is a typical fold and thrust belt (Ribeiro et al. 1979, 1983; Ribeiro and Silva 1983; Silva et al. 1990) with a slightly arcuate pattern ranging from NW–SE to a NNW–SSE trend towards W (Fig. 1A; e.g. Ribeiro et al. 1979; Dias and Basile 2013). This deformation was the result of the basin inversion induced by the SW Iberia Variscan subduction zone (Ribeiro et al. 2007). Such process generated a SW-facing imbricated complex (Fig. 1B), related to a thin-skinned tectonic regime (Ribeiro and Silva 1983; Ribeiro et al. 1983).

The lithostratigraphy of the South Portuguese Zone allows the individualization of three domains in SW Portugal (see Oliveira et al. 2013 for a review): from NE to SW, the Pyrite Belt, Baixo Alentejo Flysch Group and Southwest Sector (Fig. 1C). In the framework of this work, the Baixo Alentejo Flysch Group, a deep water turbidite sequence with more than 5-km thickness (Oliveira et al. 2013), must be highlighted. Sedimentological and palaeontological data allow the establishment of three main lithostratigraphic units in this group (Oliveira 1990): Mértola, Mira and Brejeira formations. The spatial relation of these units shows a southward propagating of the basin, from Upper Visean to Upper Moscovian (Oliveira et al. 2013; Jorge et al. 2013).

The continuous interaction between deformation and sedimentation (Ribeiro and Silva 1983) highlights a diachronous propagation of the deformation from NE to SW in a piggy back regime (Carvalho et al. 1971; Silva 1989; Silva et al. 1990). The deeper structural levels with a pervasive cleavage are thus present in the NE, while southwards a shallower deformation is found (Ribeiro et al. 1983; Marques et al. 2010; Dias and Basile 2013). The Variscan metamorphic grade reflects the structural pattern, ranging from the greenschist facies in the NE to top diagenesis/anchizone towards the SW (Schermerhorn 1971; Munhá 1983; Abad et al. 2004).

Although strongly deformed, the general pattern of the SW Variscan imbricated complex is the result of a very homogeneous stress field. This leads to considering a unique and continuous diachronous tectonic phase (Ribeiro et al. 1979; Ribeiro and Silva 1983; Caroça and Dias 2001; Marques et al. 2010; Reber et al. 2010; Zulauf et al. 2011; Dias and Basile 2013). As it is the first and main tectonic phase found in this sector, it is usually considered a local D_1 event (Ribeiro 1983; Ribeiro and Silva 1983; Silva et al. 1990; Caroça and Dias 2001; Marques et al. 2010; Dias and Basile 2013).

The understanding of the D_1 structures in the external sectors of SW Iberia is essential to the study of the more discrete and heterogeneous Late Variscan deformation (D_2) which is developed in a different geodynamical context (Dias and Basile 2013).

The first Variscan deformation phase (D_1) in SW domains of South Portuguese Zone

The D_1 structures overlap syn-sedimentary normal faults with local expression. Although they have been considered the result of an extensional regional environment leading to the deepening of the sedimentary basins (Marques et al. 2010), they could also result from flexural extension, due to bending of lithospheric plate, in the foredeep–foreland transition zones during collisional processes (e.g. Bradley and Kidd 1991; Scisciani et al. 2001).

The continuity of the shortening related to the D_1 tectonic event gives rise to a frequent superposition of

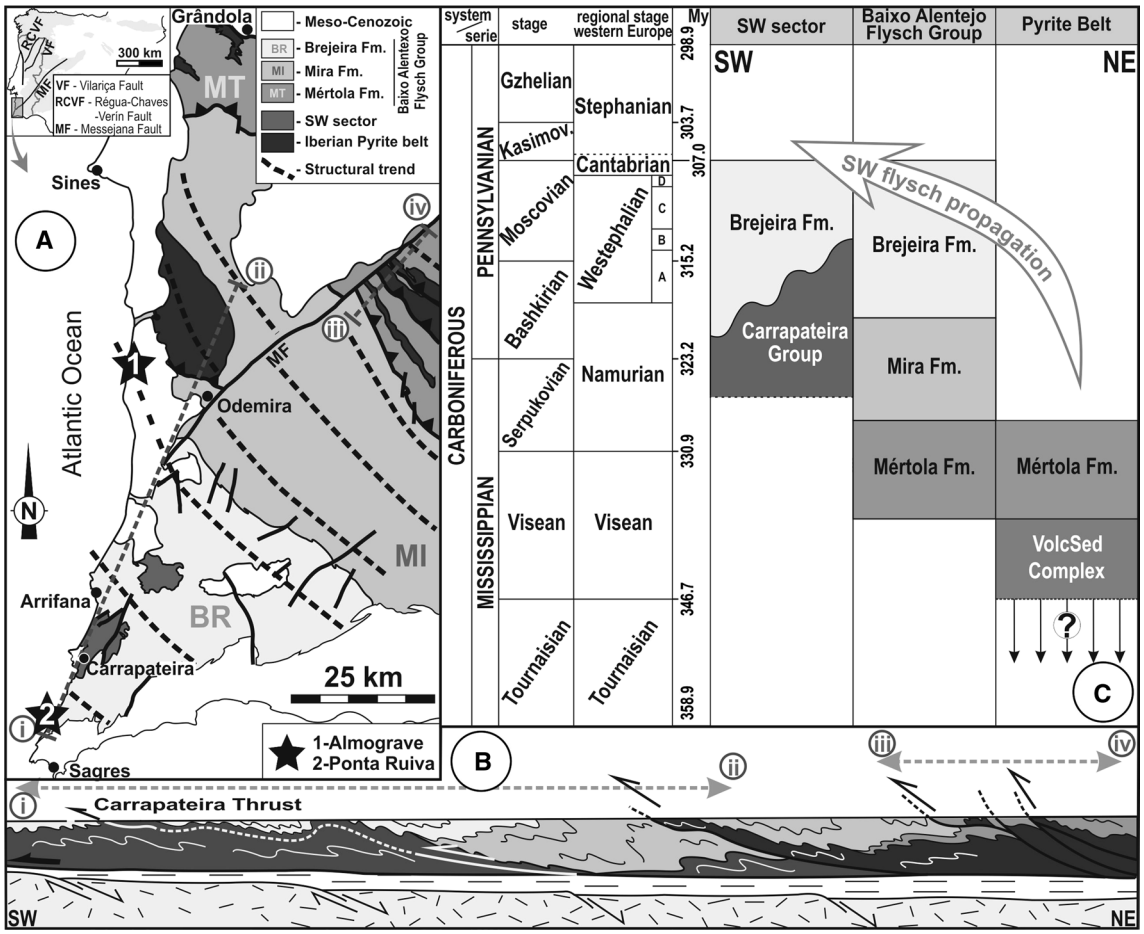

Fig. 1 Main geological features of the southern Portuguese Variscides. **A** Spatial distribution of the main geological domains (adapted from Oliveira 1984; Ribeiro et al. 1979). **B** Geological profile along the South Portuguese Zone (adapted from Ribeiro et al. 2007; location is shown in Fig. 1A). **C** Main lithostratigraphic units emphasizing the Carboniferous turbidites (adapted from Oliveira 1990; Silva et al. 1990, 2013; Oliveira et al. 2013)

mesoscopic structures with complex interference patterns. As these structures share a common stress field, they must be ascribed to the same deformation phase. Nevertheless, their well-defined geometry and kinematics made possible the subdivision of several stages.

The oldest D_1 structures (D_{1a}) were developed by layer-parallel shortening (Fig. 2A), when the layers were still subhorizontal. In the more competent quartzwacke layers, conjugated shear zones underlined by en echelon quartz veins were developed (Marques et al. 2010; Dias and Basile 2013). The trends of the conjugate dextral NNE–SSW and the sinistral ENE–WSW to E–W shear zones indicate a stress field with a subhorizontal NE–SW σ_1, a NW–SE σ_3 also subhorizontal and a subvertical σ_2. Quartzwacke boudins and extensional fractures orthogonal to σ_3 are common structures. In the pelitic layers, this early tectonic shortening was accommodated essentially by thickening.

The continuity of the compressive deformation induced general folding (D_{1b}), not only of the layers, but also of the D_{1a} structures (Fig. 2B). As expected in a SW-propagating fold and thrust belt (Carvalho et al. 1971), the vergence of these folds is towards the SW foreland. As the folds have been developed in a relatively upper structural level (Marques et al. 2010; Zulauf et al. 2011), the axial planar S_1 cleavage is only predominant in the hinge zones and reverse limbs of the D_{1b} folds, affecting preferentially the more pelitic lithologies.

Probably related to the post-buckling flattening (Marques et al. 2010), low-dipping thrusts were formed (Fig. 2C; Ribeiro 1983; Ribeiro et al. 1983; Caroça and Dias 2001; Dias and Basile 2013). Due to the out-of-sequence propagation of these thrusts (Ribeiro 1983; Ribeiro and Silva 1983), which are considered D_{1c} structures, they often cut previous D_{1b} folds (Fig. $2C_1$). In the vicinity of major thrusts (e.g. the Carrapateira nappe; Ribeiro 1983; Fig. 1B), a stretching lineation (X_{1c}) is found parallel to the top-to-SW Variscan transport. This lineation is parallel to quartz fibres in pressure shadows adjacent to pyrite crystals (Fig. $2C_2$).

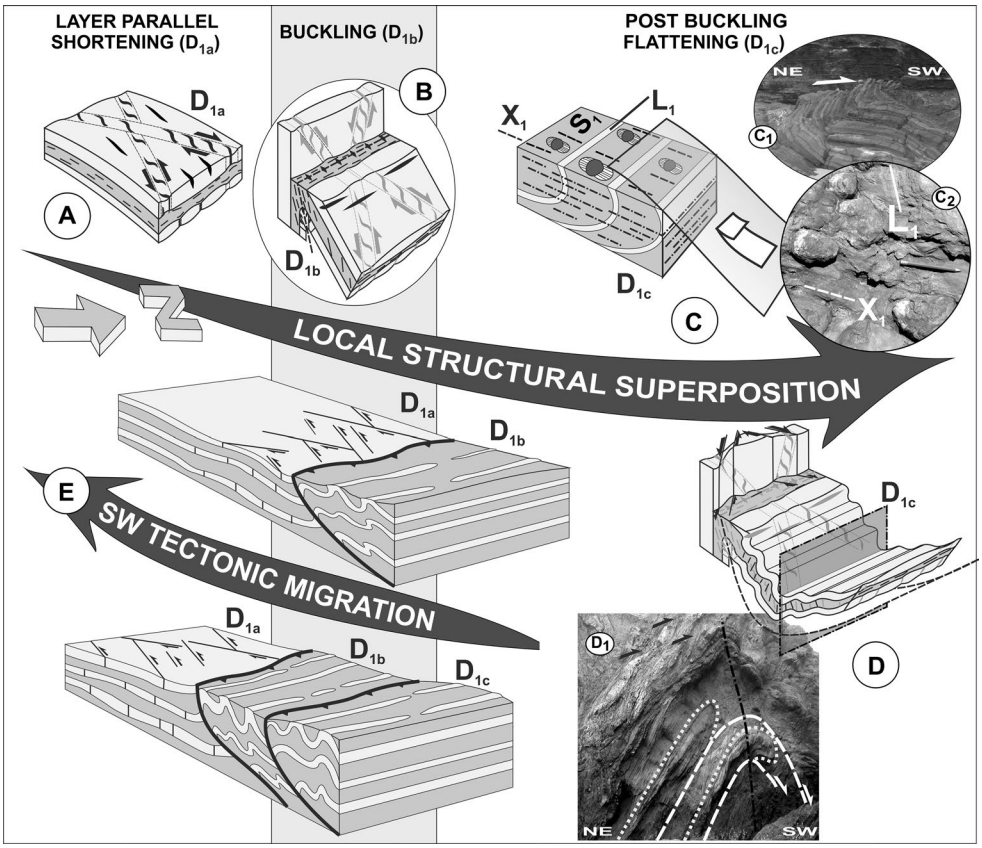

Fig. 2 Main structural features of the D_1 deformation evolution in SW Portugal (adapted from Dias and Basile 2013). **A** Conjugated shear zones and extensional fractures developed during D_{1a} layer-parallel shortening stage; **B** D_{1b} folds with outer arc extensional veins (in *black*) cutting D_{1a} en echelon quartz veins (in *grey*); **C** D_{1c} thrusts cutting previous folds (C_1 Mouranitos thrust north of Sagres) emphasizing the X_1 stretching lineation orthogonal to fold axes (C_2 quartz pressure shadows parallel to stretching lineation in Carrapateira nappe); **D** D_{1c} deformation superposed on previous D_1 folds and thrusts (D_1 in the Sagres sector); **E** diachronous D_1 SW migration

The effect of this post-buckling D_{1c} shortening on previous folds is mostly controlled by the D_{1b} geometry (Fig. 2D). In the steeply dipping short limbs, the late regional D_1 shortening produced conjugated brittle to brittle–ductile subvertical D_{1c} shear zones: N–S to NNE–SSW dextral and ENE–WSW to E–W sinistral (Caroça and Dias 2001; Marques et al. 2010). In the low-dipping D_{1b} normal limbs and early D_{1c} thrusts, the late shortening mostly induced the formation of open to tight folds with subvertical axial planes and subhorizontal fold hinges, which refolded the older structures (Fig. 2D_1; Caroça and Dias 2001).

Although the use of previous D_1 deformation stages is useful at local scale, care should be taken at the regional level due to the diachronous propagation of the deformation (Fig. 2E).

Variscan geometry and kinematics at external domains of the South Portuguese Zone

In order to improve the knowledge of the Late Variscan deformation in SW Iberia, two sectors have been chosen: Almograve and Ponta Ruiva (Fig. 1A). While in Almograve, it is possible to detail the superposition of different stages related to the Variscan deformation, in Ponta Ruiva, their relation with the extensional Triassic events, due to the opening of the Atlantic Ocean, can also be studied.

The Almograve sector

The most evident structures in Almograve are the sudden regional D_1 strike changes by decametric to hectometric NNE–SSW brittle to brittle–ductile kink bands (Fig. 3). Although well exposed, its genesis is debatable (Caroça and Dias 2002; Marques et al. 2010; Dias and Basile 2013).

Structural pattern of Almograve sector

Concerning the Variscan major structure of Almograve, there is a strong contrast between the NNW–SSE bedding trend domains and the WNW–ESE to E–W ones (Fig. 3).

Variscan folds In the NNW–SSE segments (Fig. 4A, B), although the D_1 folds have sometimes complex shape profiles due to rheological contrasts of the turbiditic multilayer (Fig. 4B) and intense fluid migration (Marques et al. 2010), they have a very regular, N20°W–N30°W trend (Fig. 4A_1, B_1, C_1), which is also the direction of the locally developed axial planar S_1 cleavage (Fig. 4A_2, B_2). When present, the L_1 intersection lineation (S_0^S_1) is subhorizontal or very low dipping to NNW (usually <10°), being subparallel to the

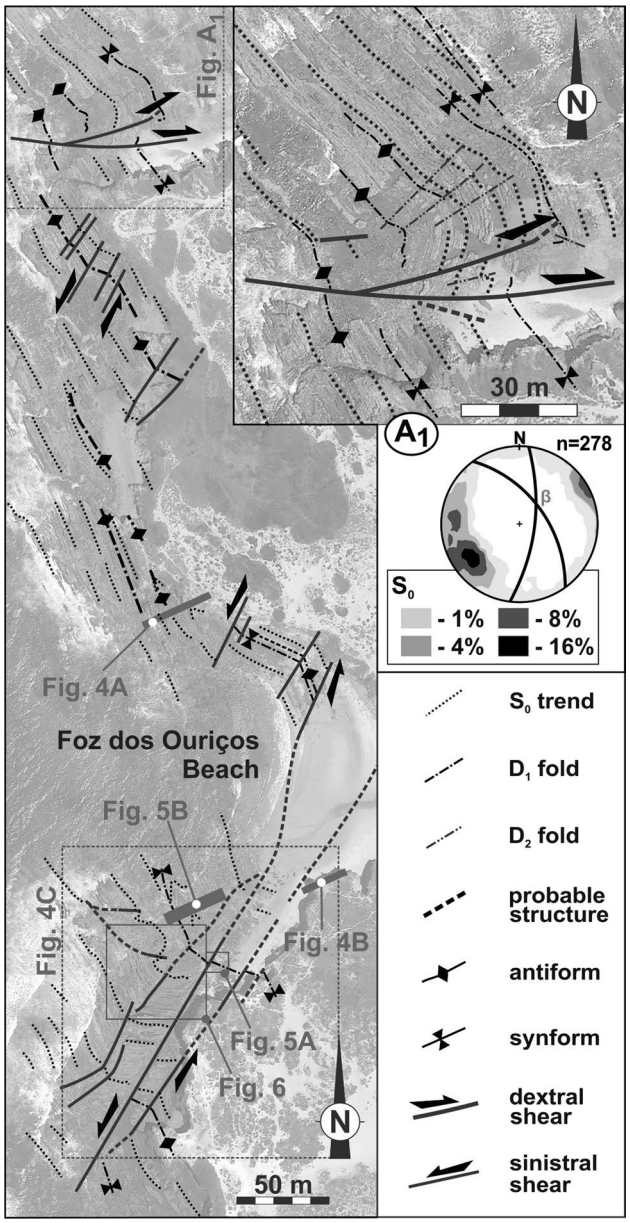

Fig. 3 General Variscan structural map for the Almograve-Foz dos Ouriços area. The *inset* (A_1) shows structural details of northern sector

fold hinges (Fig. 4A_2, B_2). As the axial planes are subvertical, the folds in Foz dos Ouriços/Almograve have no clear vergence, although immediately SW of the studied domain the SW vergence is well expressed (Dias and Basile 2013).

The Variscan folds in the WNW–ESE to E–W sectors have a much more complex geometry due to the pervasive superposition of a different folding event. The pattern of these post-D_1 folds is highly heterogeneous due to the coexistence of two completely different set of D_2 folds, which are easily distinguishable by their symmetry in an orthorhombic (Fig. 5) and a monoclinic set (Fig. 6).

The orthorhombic D_2 folds (Fig. 5) have a NNE–SSW to NE–SW trend and variable axes, which were mostly controlled by the dip of the D_1 fold limbs (Fig. 5A_1, B_1). The weak flattening related to these D_2 folding led to the development of an incipient S_2 crenulation cleavage, which is usually restricted to the more pelitic layers. When present, the S_2 cleavage (Fig. 5A_1, B_2) is axial planar giving rise to a L_2 (S_0^S_2) intersection lineation parallel to D_2 hinges (Fig. 5A_2, B_2).

As both the D_1 and the D_2 orthorhombic folds have subvertical axial planes and subperpendicular trends, a type 1 fold interference (Ramsay and Huber 1987) was produced.

Although the D_2 orthorhombic folds are common in most of the WNW–ESE kinked domains, they are more frequent in the vicinity of the NNE–SSW faults that bound them. This shows that such folds were developed due to the movement along these faults. The slight obliquity between the NE–SW folds and the N30°E fault is compatible with a sinistral kinematics along the NNE–SSW trend. Such conclusion is also supported by previous works in other sector of SW Portugal (Caroça and Dias 2002) that described en echelon NE–SW D_2 folds transected by an ENE–WSW S_2 cleavage, indicating a sinistral kinematics associated with NE–SW shear bands.

Concerning the monoclinic D_2 folds set (Fig. 6), they are only found when the layers have strong dips and a trend close to E–W. They are also typical of places where the turbidites have a predominance of shales interbedded with centimetric to decimetric quartzwackes, often in the vicinity of metric quartzwacke layers not affected by such folding. These D_2 folds have subvertical axial planes slightly oblique to bedding trend, strongly plunging hinges and an eastern facing (Fig. 6B_1). This geometry is compatible with a dextral shearing along the bedding. This is kinematically consistent with the subhorizontal slickensides in the bedding planes (Fig. 6B_2), coupled with other sense of movement indicators, like sigma-shaped competent bodies (Fig. 6B_3) or dextral faults (Fig. 6B_4) often nucleating in the short limbs of these D_2 folds (Fig. 6B_5).While the monoclinic D_2 folds are pervasive in the inner domain of Foz dos Ouriços Kink, when approaching from its boundaries previous anisotropies where sometimes reworked with a sinistral kinematics along NNE-SSW trend (Fig. 6C).

Although both sets of D_2 folds are found in the WNW–ESE domain of the Almograve-Foz dos Ouriços kink band, due to the different genetic mechanisms, they were never observed in the same place. The absence of interference structures between both kinds of fold makes it difficult to determine their relative ages.

Variscan shear zones One of the most remarkable structures of Almograve is conjugated en echelon quartz veins related to the Variscan shear zones affecting quartz (Caroça and Dias 2002; Marques et al. 2010; Reber et al. 2010;

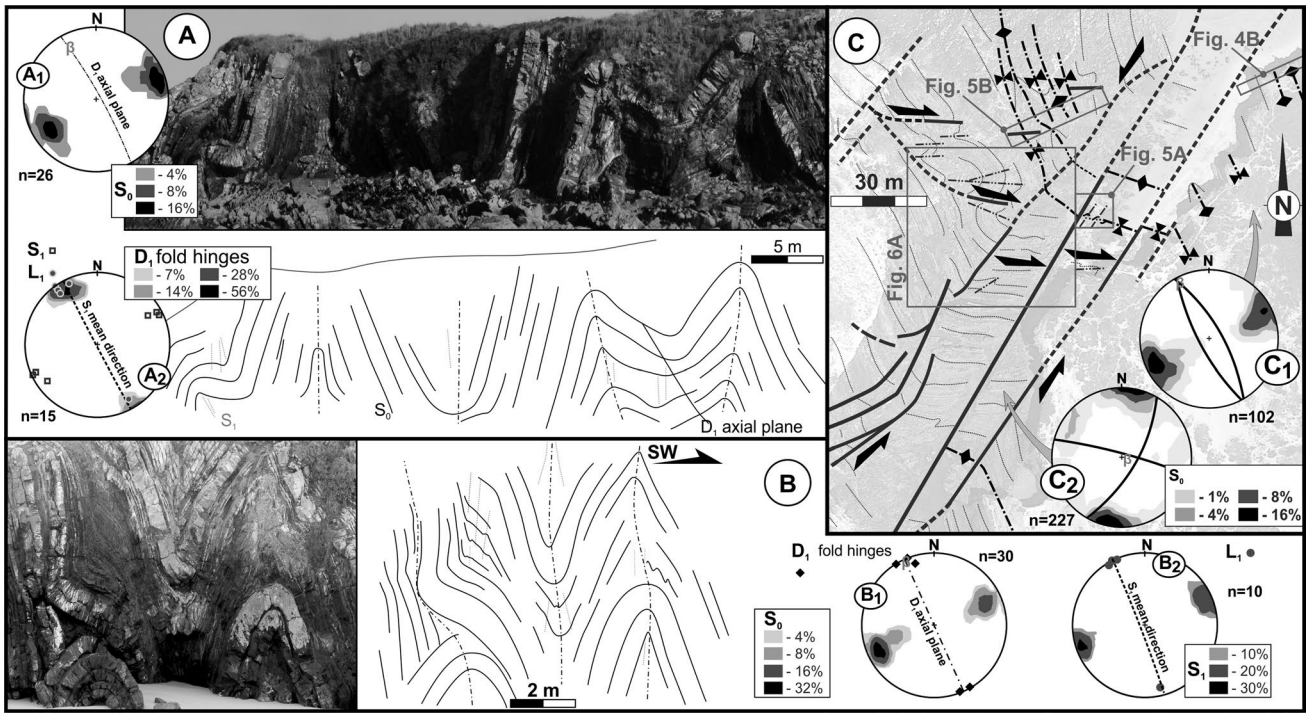

Fig. 4 Main geometry features of Variscan folds for the Almograve-Foz dos Ouriços beach NNW–SSE sectors (equal area lower hemisphere stereographic projections). **A** Fold array and geometrical data (A_1-bedding; A_2–D_1 fold hinges) in northern Foz dos Ouriços; **B** fold array and geometrical data (B_1–D_1 fold hinges; B_2–L_1 intersection lineation) in southern Foz dos Ouriços; **C** structural map of southern Foz dos Ouriços sectors with bedding stereographic analysis (symbols as in Fig. 3)

Zulauf et al. 2011; Dias and Basile 2013). According to their temporal relation with the folds, they could be classified into two different sets: the early D_{1a} veins deformed by the regional folding (Fig. 7A) and the younger ones which have been superposed on the folds (Fig. 8A). Both families could also be distinguished by their geometries. While the acute angle between the older pre-folding conjugated shear zones is very small (23°–31°; Fig. 7B), in the younger post-folding veins such angle is always close to 60° (Fig. 8B). The unusual small angle between the pre-folding conjugated shear zones is not restricted to the Almograve sector and is the rule in the SW Iberia Variscides (Fig. 7C, D).

The temporal relation between the younger shear zones and both Variscan folding events (D_1 and D_2) is easy to establish. Indeed, the pattern of the stress field deduced by the conjugated shear zones in Almograve is consistently deflected by the D_2 major kink folds (Fig. 8B): i.e. anticlockwise rotation in the E–W to WNW–ESE segments and clockwise in the NE–SW ones (Fig. 8C). The conclusion that these shear zones are pre-D_2 structures is also consistent with the fact that in each place where the stress field has been determined, the maximum principal compression (σ_1) stress is always orthogonal to the local fold trend (Fig. 8B). Thus, the younger shear zones should be considered D_{1c} according to previous nomenclature (Fig. 2).

The preservation of the stress field during the D_1 Variscan structures shows a progressive and coaxial behaviour. However, if the orientation of the principal axes is preserved, the relative intensities between the main stresses change during the evolution of D_1 deformation (Table 1). In the early D_{1a} stages, the acute angle is always below 40° (Fig. 7A), indicating the presence of hybrid fractures (Belayneh and Cosgrove 2010) formed in a very low D_{1a} differential stress (σ_1–σ_3; Price and Cosgrove 1990; Cosgrove 2005). The acute angle is always constant and close to the normal 60° for the late D_{1c} conjugate shears (Fig. 8B) expressing a higher differential stress (Belayneh and Cosgrove 2010). Such a difference seems to be indicating that during the D_{1c}, the deformation occurred at a higher structural level than during D_{1a}, which could result from the thickening of the turbiditic sequence due to the Variscan deformation. Indeed, the smaller D_{1a} acute angles could not be explained by the superposition of the flattening of younger D_{1b} or D_{1c} Variscan deformation events, because the similar orientation of their stress fields should have increased the initial angle whatever the limb in which they are found.

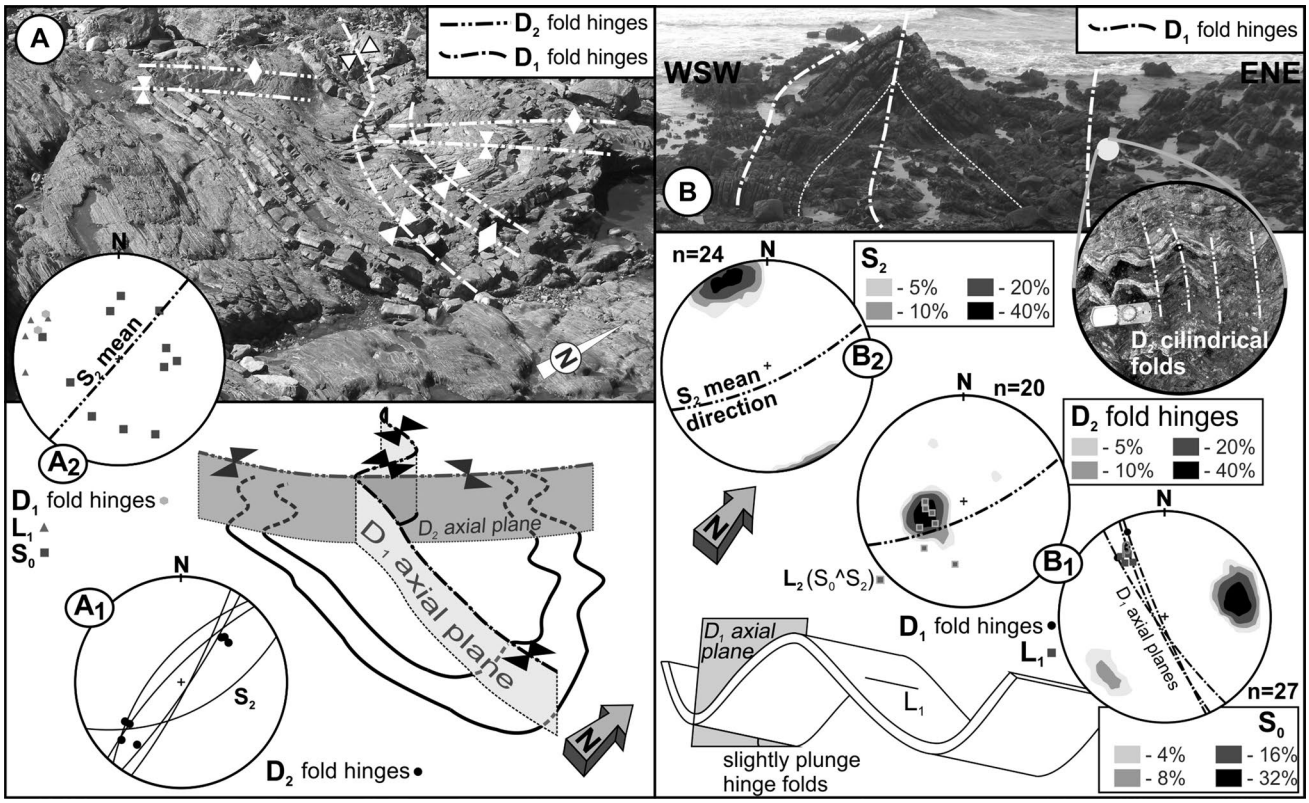

Fig. 5 NNE–SSW orthorhombic D_2 structures in the E–W Almograve sector (equal area lower hemisphere stereographic projections). **A** Wavy D_2 hinges in a D_1 syncline refolded by D_2 folds; **B** moderate NNW dipping of D_1 folds overprinted by D_2 folding

Variscan kinematics of the NNE–SSW fault trend

The kinematics and age of the NNE–SSW major Variscan strike-slip faults in SW Portugal have been explained by two different opposite models:

- dextral and contemporaneous of the main D_1 regional folding event (Marques et al. 2010; Fig. 9A);
- sinistral and younger than the main D_1 regional folding event (Caroça and Dias 2002; Ribeiro et al. 2007; Dias and Basile 2013; Fig. 9B).

In the first model, the NNW–SSE structural trend is the result a local clockwise drag of the regional NW–SE structures due the dextral shearing along the major NNE–SSW wrench faults. This rotation, which was contemporaneous of the main D_1 folding event, gave rise to the E–W monoclinic folds, by a flattening mechanism induced by the interference between the regional compression and the dextral kinematics along the NNW–SSE layers (Fig. $9A_1$). Such dextral shearing was supported either by en echelon quartz veins, or the deflection of sand dykes (figure 8 of Marques et al. 2010). Concerning the quartz veins, care should be taken because described geometry is also compatible with both dextral D_{1a} (Fig. 2A) and D_{1c} shears (Fig. 2D). Regarding the sand dykes, although they are usually considered to have initiated as orthogonal fractures to subhorizontal layers during diagenetic compaction (Cosgrove 1997), field examples show that often they initiate oblique to the layering. This is clearly demonstrated by the coexistence in the same place of sand dykes with opposed deflections (Fig. 10). This strongly argued against the use of sand dykes as kinematic markers.

It should be enhanced that although the dextral kinematics along NNE–SSW faults could explain the ENE–WSW monoclinic folds (Fig. 6), it is unable to explain the frequent NE–SW orthorhombic folds (Fig. 5).

Moreover, the location of the younger D_2 structures only in the WNW–ESE kinked segment shows that this orientation has only a local significance. Thus, the NNW–SSE general trend in Almograve, where only the D_1 structures are found, must be considered the dominant regional trend, which has been anticlockwise-deflected to WNW–ESE by the sinistral kink band mechanism (Fig. 9B). Assuming such sinistral kinematics along the NNE–SSW faults, all the diversity of the structures found in Almograve could be explained (Fig. 9C). Indeed, the strong distortion related to the 57° rotation of the kink band inner domain in relation

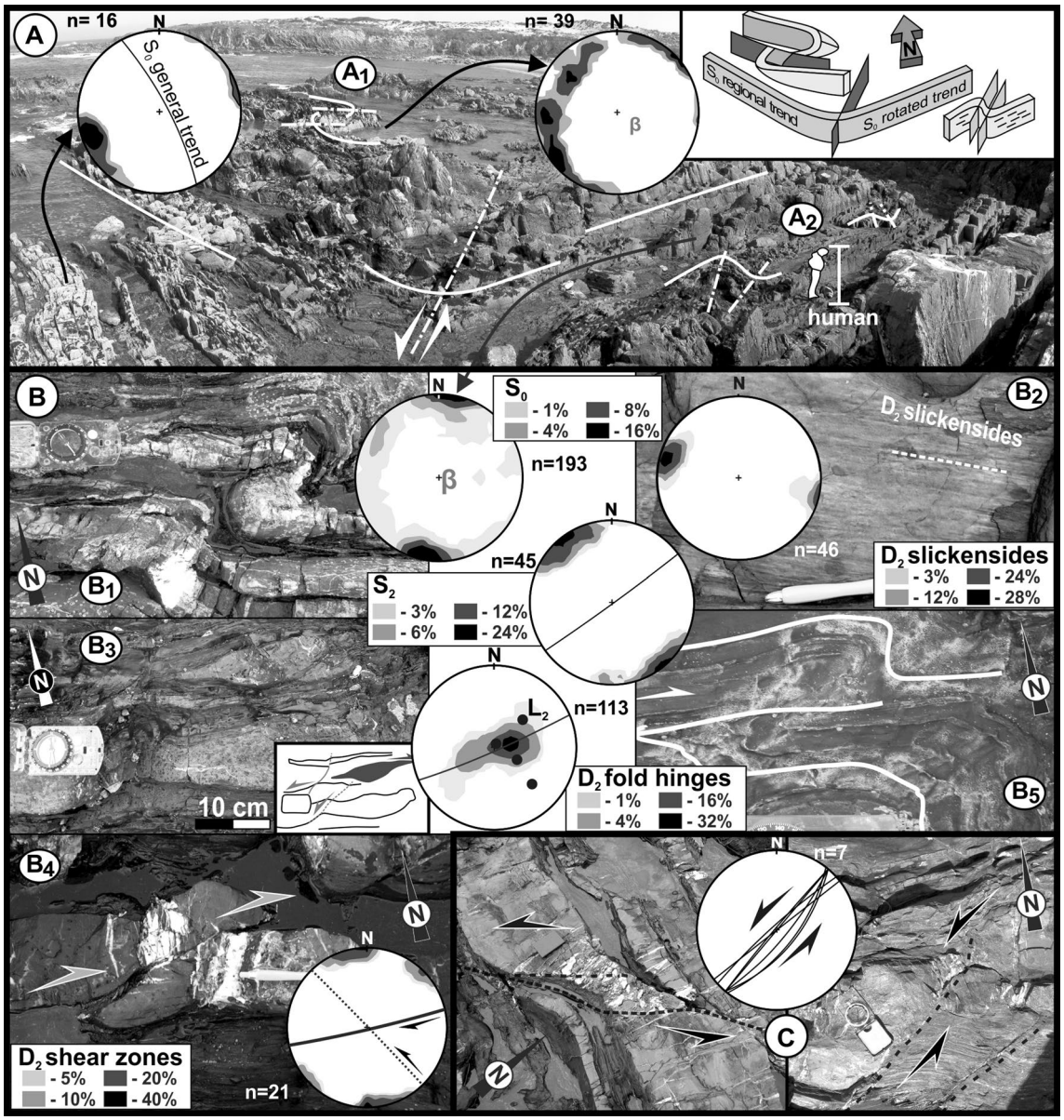

Fig. 6 Geometrical and kinematical features related to D_2 monoclinic structures in the E–W Almograve sector (equal area lower hemisphere stereographic projections). **A** Western boundary of the main Foz dos Ouriços kink band (see Fig. 4A for location); **B** E–W D_2 dextral shear structures; **C** NNE–SSW D_2 sinistral shears

with the outer NNW–SSE regional trend, superimposed on a highly anisotropic material, gave rise to the coexistence of different deformation mechanisms. Considering a constant width of the kink band (which is supported by the observation in the sectors near its extremities), and using the trends of the inner and outer domains, a 20% shortening should be expected during the rotation (Fig. 9C_1). Thus, the simple and rigid rotation of previous D_1 structures (Fig. 9C_2, C_3) cannot accommodate all the Late Variscan deformation inside the shear zone. As there is no evidence of considerable volume loss related to the D_2 phase (e.g. the intense quartz veining of Almograve is only related to the D_1 deformation), this orthogonal shortening must be compensated by subhorizontal and/or subvertical extension. The deformation induced by this shortening is heterogeneously distributed, being stronger in the vicinity of the kink band subvertical boundaries. The NNE–SSW to NE–SW D_2 folding with orthorhombic symmetry (Fig. 5) as well as conjugated shears displacing layer boundaries is due to such mechanism (Fig. 9C_4). The lack of vergence of these folds is explained by the subvertical geometry of the kink band limits which behaves as obstacles to the migration of the D_2 deformation.

The D_2 folds with subvertical hinges and a strong monoclinic symmetry highlight a strong dextral shearing

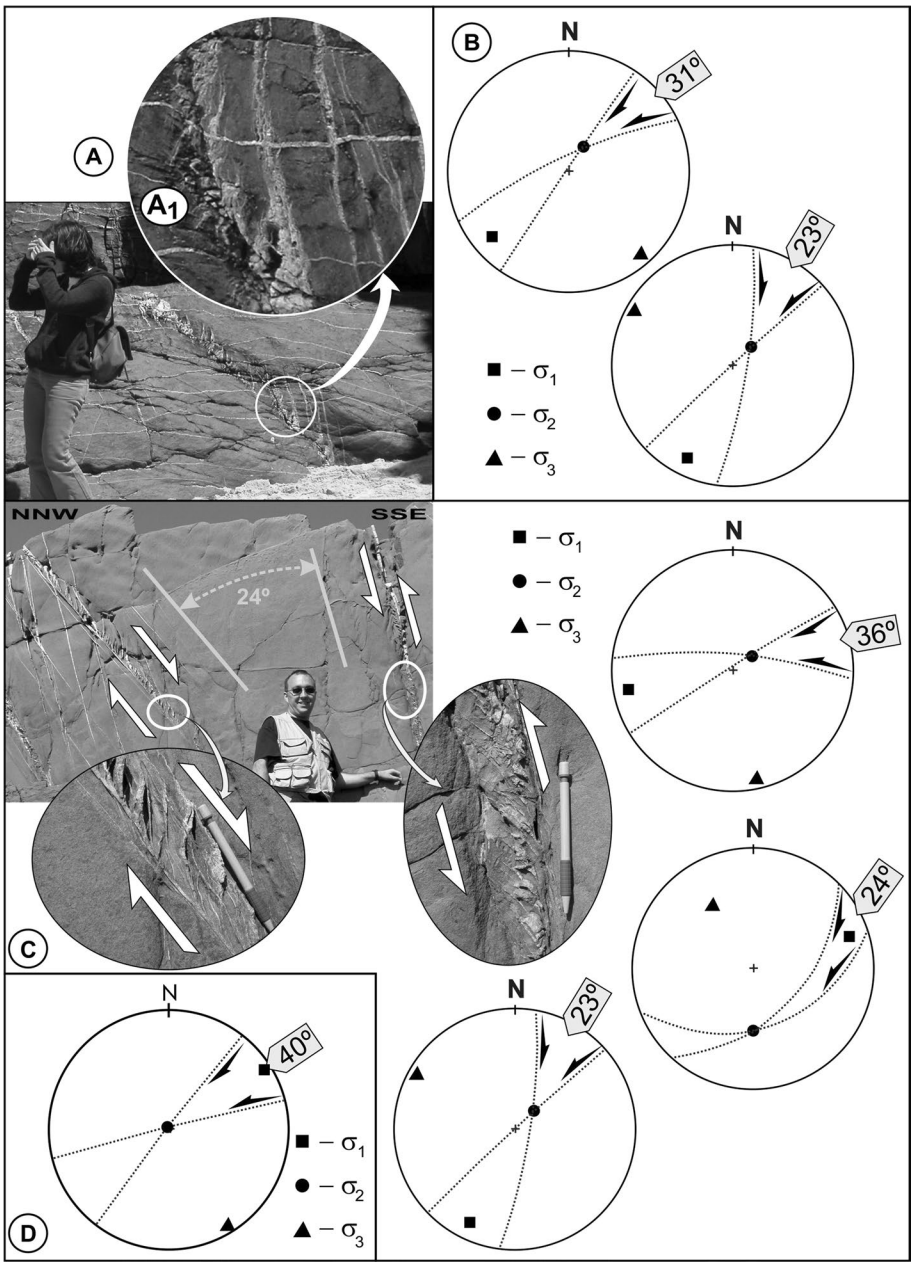

Fig. 7 Geometric and kinematic features of older conjugated Variscan shear zones in SW Iberia coast (equal area lower hemisphere stereographic projections): **A** En echelon quartz veins cut by outer arc fold extensional veins developed in Foz dos Ouriços beach folds (A_1); **B** conjugated shear zones and related stress field for two situations in the southern domain of Almograve; **C** conjugated shear zones and related stress field in the Arrifana sector; **D** conjugated shear zones and related stress field for Cachado sector (north of Sagres)

subparallel to layers in the WNW–ESE inner domain (Figs. 6B, 9C_5), this is an expected behaviour in some sinistral kink band (Ramsay and Huber 1987; Twiss and Moores 1992). Indeed, the progression of the sinistral rotation of the kink should be coupled with dextral shear strain on the rotating surfaces (Fig. 9C_5, C_6).

The heterogeneities of the turbidite sequence could induce some irregularities in the structural pattern. The anomalous major fold (Figs. 6A_1, 9C_7), although presenting a geometry similar to the D_2 monoclinic folds, is located outside the inner domain of the kink bands is attributed to the indentation of an anomalous metric thick quartzwacke package in adjacent pelitic zones (Fig. 9C_8). Indeed, the shortening of such a competent package inside the kink band is difficult due to space considerations, which induce its indentation in the sectors adjacent to the kink band where incompetent shales are predominant. Such mechanism will produce not only the folding/disruption of the boundaries of the kink band, but also anomalous folding in the domains adjacent to the indentor (Coke et al. 2003).

It is worth noticing that in Northern domains of the studied Almograve sector (Fig. 3), an important E–W dextral shear zone is found in places not related to sinistral kink

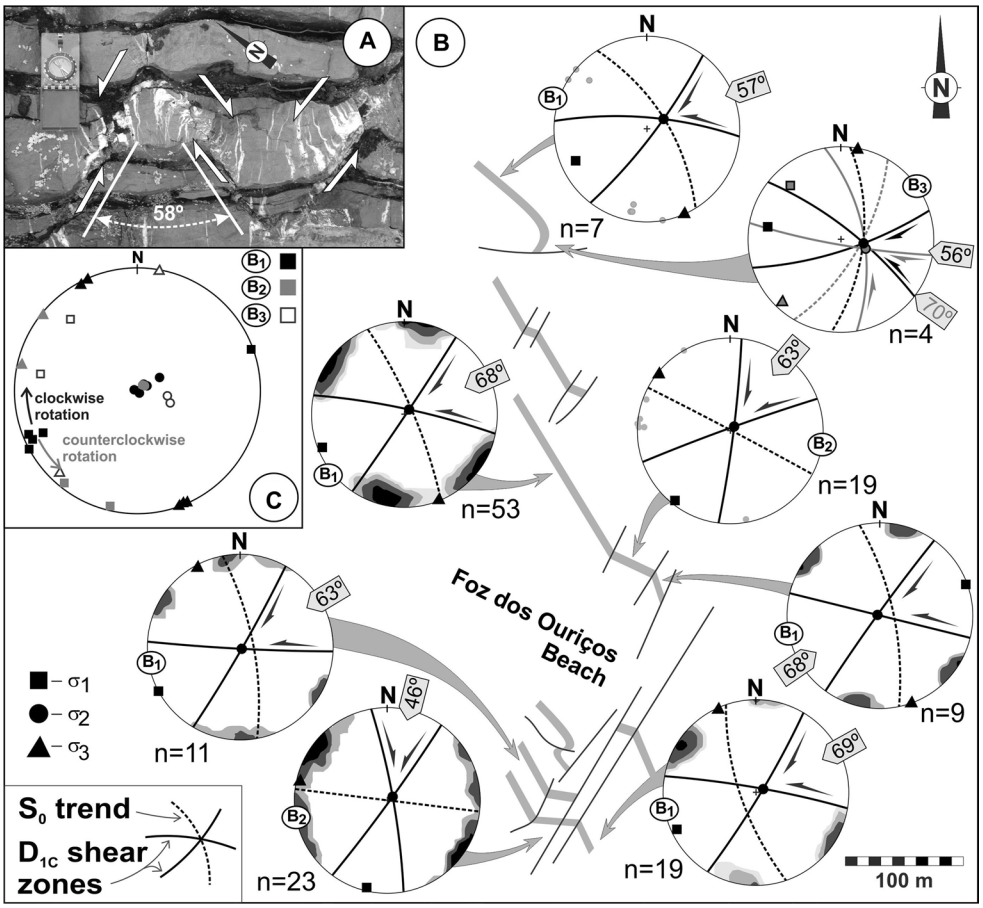

Fig. 8 Geometric and kinematic features of younger conjugated Variscan shear zones in Almograve (same area of Fig. 3): **A** conjugated shear zones displacing strongly dipping layers of Almograve sector; **B** conjugated shear zones and related stress field for several situations in the Almograve domain (equal area lower hemisphere stereographic projections); **C** compilation of Almograve stress field data

Table 1 Conjugated D_1 shear zones in SW Portugal

Sector	Tectonic event	Shear A		Shear B		Angle	σ_1	σ_2	σ_3
		Attitude	Kinematics	Attitude	Kinematics				
Almograve	D_{1c}	N40°E, 90	Dextral	N80°W, 90	Sinistral	60°	0°, N70°E	90°	0°, N20°W
Almograve	D_{1c}	N25°E, 80°W	Dextral	EW, 70°N	Sinistral	63°	7°, S60°W	70°, N8°W	18°, S33°E
Almograve	D_{1c}	N80°E, 75°N	Sinistral	N27°E, 75°E	Dextral	58°	32°, S52°W	58°, N54°E	2°, N37°W
Almograve	D_{1a}	N37°E, 90°	Dextral	N68°E, 84°S	Sinistral	31°	20°, S50°W	70°, N35°E	5°, S42°E
Almograve	D_{1a}	N56°E, 52°S	Normal	N62°E, 7°4S	Reverse	23°	33°, N37°E	56°, S51 W	6°, S48°E
Arrifana	D_{1a}	N68°E, 33°S	–	N56°E, 68°S	–	36°	14°, S78°W	75°, N54°E	5°, S13°E
Arrifana	D_{1a}	N63°E, 53°S	Normal	N65°E, 77°S	Reverse	24°	20°, N71°E	47°, S3°W	37°, N35°W
Arrifana	D_{1a}	N54°E, 83°N	Sinistral	N14°E, 80°N	Dextral	40°	14°, S28°W	74°, N40°E	4°, N62°W
Cachado	D_{1a}	N77°E, 78°N	Sinistral	N40°E, 76°N	Dextral	36°	4°, N58°E	86°, S80°W	1°, S32°E

bands. This shear zone generates a decametric drag fold, with NE–SW subvertical axial plane and steeply plunging hinge (Fig. 3A$_1$), which rotate previous structures (Fig. 8B), showing that it is also related to the Late Variscan D_2 episode.

The Ponta Ruiva sector

In Ponta Ruiva, the angular unconformity between the weakly deformed Triassic sediments and the highly folded low metamorphosed Carboniferous units is exceptionally

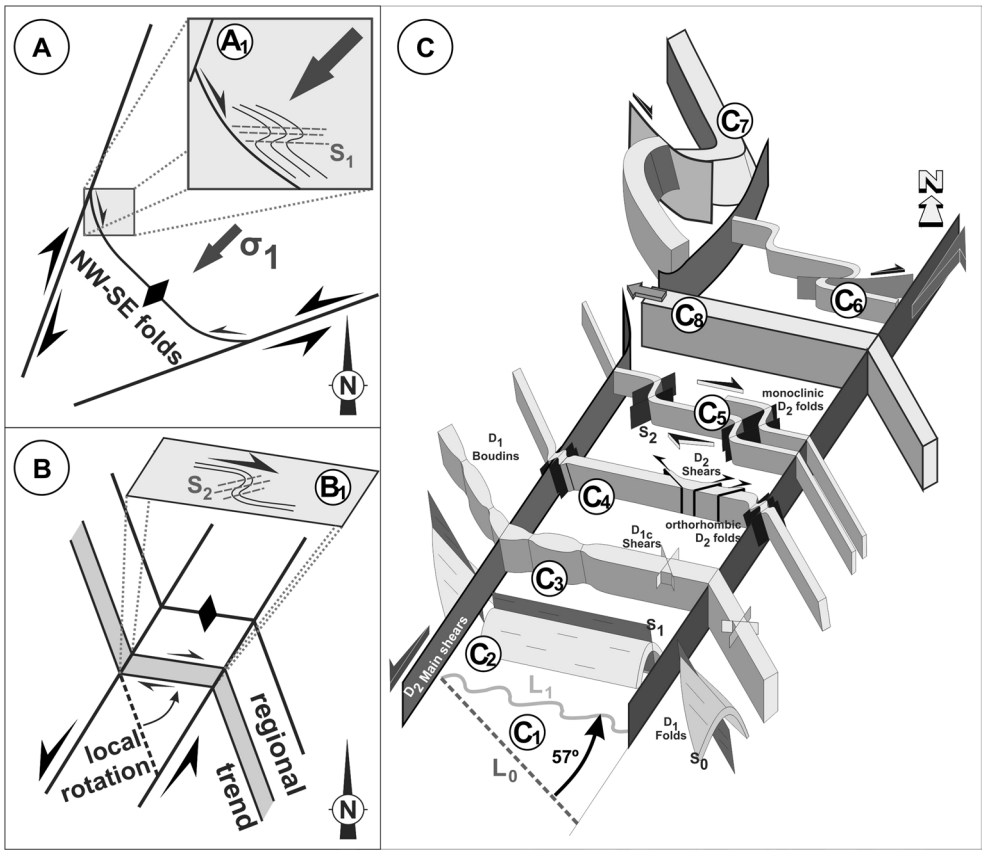

Fig. 9 Geometry and kinematics related to the NNE–SSW structures in SW Portugal. **A** The dextral model (adapted from Marques et al. 2010); **B** the sinistral model (adapted from Caroça and Dias 2002; Dias and Basile 2013); **C** main structural features related to the Foz dos Ouriços kink band (see text for more details)

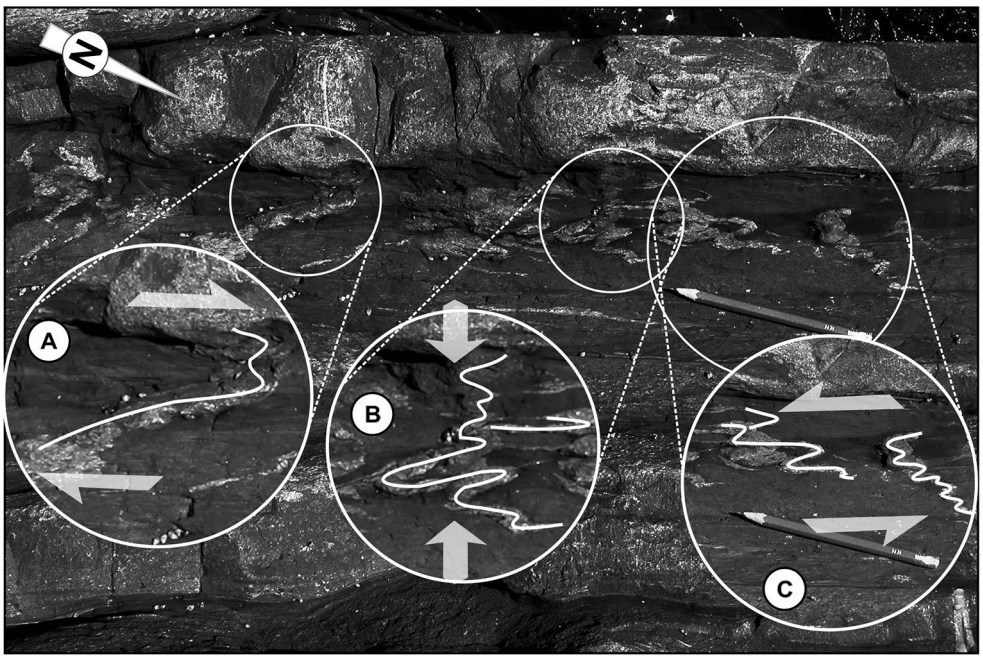

Fig. 10 Geometric complex behaviour of sedimentary dykes induced by diagenetic compaction in Arrifana port region. **A** Apparent dextral kinematics; **B** orthogonal flattening; **C** apparent sinistral kinematics

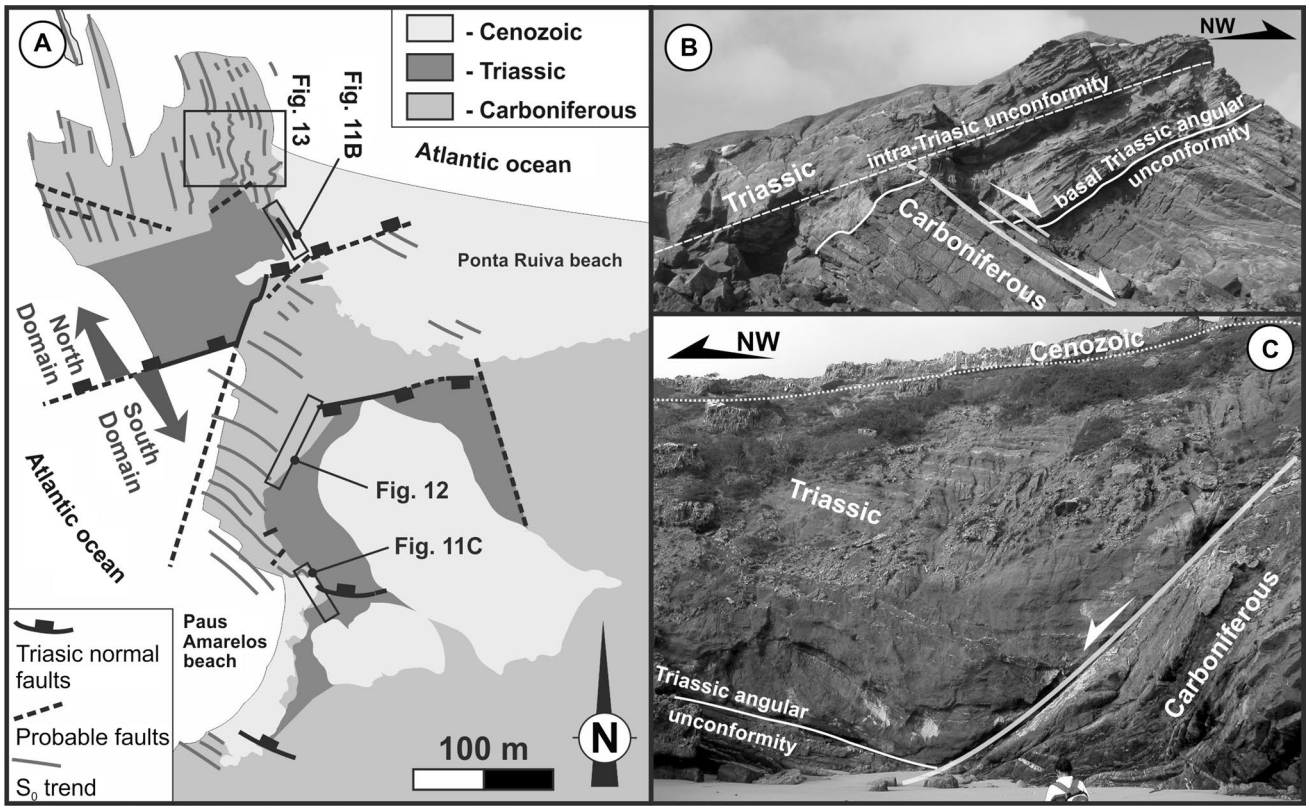

Fig. 11 General structural pattern of Ponte Ruiva area. **A** Structural map emphasizing main features related to D_2 deformation; **B** Triassic unconformity of the northern domain; **C** Triassic unconformity and extensional boundary fault of southern domain

exposed (Fig. 11). As in Almograve, in Ponta Ruiva it is possible to observe adjacent sectors with contrasting Variscan trends (Fig. 11A): NNW–SSE and NW–SE. However, here the transition between both domains is harder to understand, not only due to a strong overprinting by the early episode related to the Atlantic opening, but also to the smaller extent of the outcrops in the wave-cut platform. This younger extensional tectonic event gives rise to a complex set of small-scale intracontinental basins filled by several syn-rift sedimentary units of Triassic age (Dias and Ribeiro 2002). The opening of these basins has been controlled by the reworking of previous Variscan anisotropies (Dias and Basile 2013) with ENE–WSW to E–W trend.

Variscan deformation geometry in Ponta Ruiva sector

The geometry of the Variscan deformation in the Carboniferous turbidites led to the individualization of two different domains in Ponta Ruiva (Fig. 11A).

- The southern domain is well expressed along the cliffs and the neighbouring wave-cut platform. The main structure (Fig. 12) corresponds to a major NW–SE D_1 recumbent fold facing to SW with subhorizontal axial plane (Fig. 12A). The S_1 cleavage (Fig. 12B), which fans around the fold, is pervasive in the more pelitic layers. It has an axial plane attitude which is also confirmed by the parallelism between the subhorizontal L_1 (S_0^S_1) intersection lineation and the D_1 fold hinges (Fig. 12C). Locally, rare D_2 folds occur with subvertical axes (Fig. 11D), which are more frequent in the vicinity of the major extensional fault of the Paus Amarelos beach (Fig. 11C).
- The northern domain corresponds to the more external sector of the wave-cut platform, where the Variscan structure is a reverse limb of a major D_1 fold. The singularity of this domain in the regional context comes not only from the NNW–SSE trend (Fig. 13A), but mostly from the dipping hinges of the minor D_1 folds (Fig. 13B, C). The present attitude of the fold axes (26°, N44°W; Fig. 13C) would increase the plunge when the pre-Triassic position is restored by the removal of the Atlantic extensional deformation (37°, N52°W; Fig. 13D). The plunging hinges of the D_1 mesoscopic folds show that the Variscan geometry of this domain is local and results from the distortion of the regional structure where the folds have always subhorizontal hinges, as observed in the southern domain (Ribeiro and Silva 1983; Silva et al. 1990; Dias and Basile 2013).

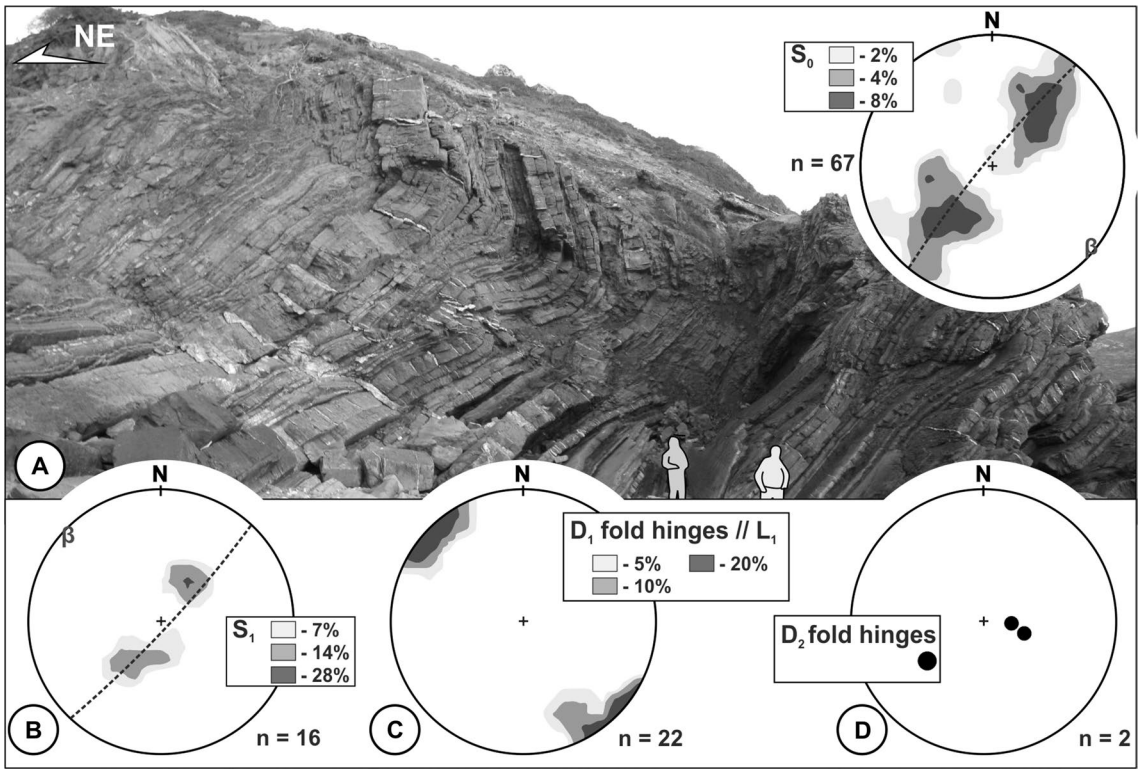

Fig. 12 Structural features in the southern domain of Ponta Ruiva (equal area lower hemisphere stereographic projections): **A** main D_1 recumbent fold with bedding (S_0) geometry; **B** S_1 cleavage geometry; **C** geometry of L_1 intersection lineation and D_1 hinges; **D** geometry of D_2 hinges

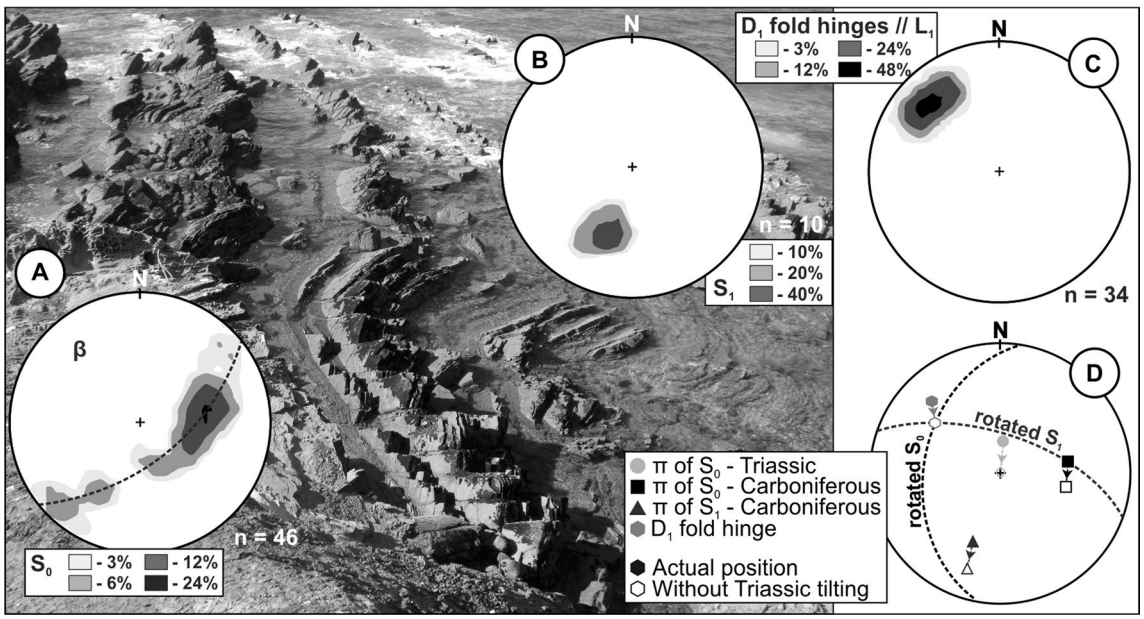

Fig. 13 Structural features in the northern domain of Ponta Ruiva (equal area lower hemisphere stereographic projections): **A** D_1 folds with bedding (S_0) geometry; **B** S_1 cleavage geometry; **C** geometry of L_1 intersection lineation and D_1 hinges; **D** rotation of D_1 structures associated with the removal of the Triassic deformation

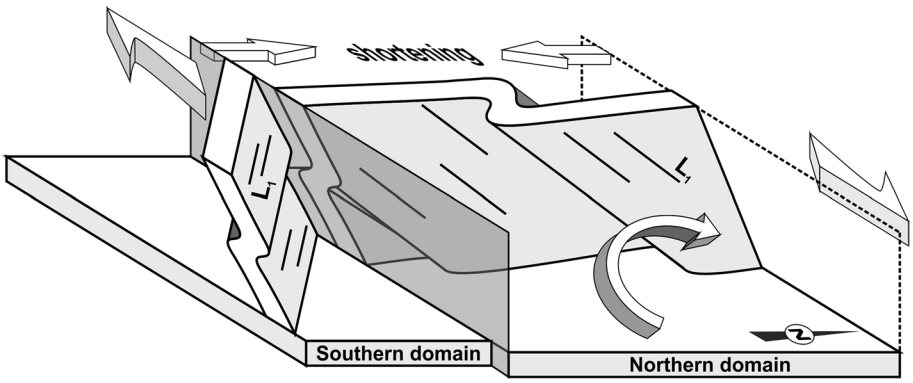

Fig. 14 Distortion of the D_1 structures by the Late Variscan ENE–WSW dextral shear

Structural evolution of Ponta Ruiva sector

The oldest structures of Ponta Ruiva are the NW–SE D_1 recumbent folds facing SW (Fig. 12A), which is the normal regional trend for the major Variscan folds in SW Portugal (Fig. 1; Ribeiro et al. 1979). The dip of the axial surfaces is controlled by the proximity to major thrusts (Ribeiro 1983), and the subhorizontal geometries observed in Ponta Ruiva results from the vicinity of D_1 major thrusts, which are frequent in SW Portugal (Fig. 1B; Dias and Basile 2013).

The local rotation of the D_1 Variscan structures observed in the northern Ponta Ruiva domain (Fig. 11A) could not be explained by the Triassic extension and must have been induced by the Late Variscan deformation, which also produced the D_2 folds with subvertical axes (Fig. 12D). The ENE–WSW to E–W trend of the major boundary faults of Ponta Ruiva Triassic basins (Fig. 11A) suggests that such direction must have been dominant during Palaeozoic times. A dextral kinematics along the ENE–WSW boundary fault between the northern and southern domains (Fig. 14), similar to the Almograve Late Variscan behaviour (i.e. Fig. $3A_1$), with the expected coeval shortening in the rotated northern sector, explains not only the more northerly trend but also the plunging hinges of the D_1 structures.

The erosive processes, which became predominant after the last increments of the Variscan deformation, gave rise to a subhorizontal surface that is well preserved at the base of the Triassic sediments (Fig. 11B, C). The structural mapping of the Triassic–Carboniferous relations shows that the Ponta Ruiva basins opening was mostly controlled by E–W to ENE–WSW normal faults (Dias and Ribeiro 2002), which locally reworked D_2 dextral strike-slip Late Variscan faults.

Geodynamical implications

The new data from the SW Iberia help the understanding of Late Variscan geodynamical evolution. Indeed, they can be used to debate the kinematics of NNE–SSW Iberian wrench faults, described in North of Portugal (e.g. Ribeiro 1974; Ribeiro et al. 1990; Lourenço et al. 2002; Marques et al. 2002; Ribeiro et al. 2007), and also constrain their deformation ages.

The deformation ages of SW Iberia structures

The older formation outcropping in the Almograve (Fig. 4) and Ponta Ruiva (Fig. 10) studied regions belongs to the Baixo Alentejo Flysch Group (Oliveira 1990). Detailed palaeontological studies (Pereira et al. 2007; Oliveira et al. 2013) show that this turbiditic formation is diachronous, ranging from Visean in the northern domains to Upper Moscovian in the southern tip. The palaeocurrent indicators preserved in the turbidites (e.g. groove and flute casts) are often subperpendicular to the D_1 fold axes, which suggests that the sedimentation is coeval with the deformation (Oliveira 1990; Dias and Basile 2013). So, the main Variscan deformation of the Carboniferous turbidites (D_1) seems to be also diachronous, being older in the more internal NE domains (Ribeiro and Silva 1983).

The age of the D_2 dextral shear zones could only be constrained in the Ponta Ruiva sector. The Carboniferous turbidites are here Upper Moscovian (Pereira et al. 2007; Oliveira et al. 2013) and have been strongly folded during D_1 (Figs. 12A, 13A; Caroça and Dias 2001; Dias and Ribeiro 2002; Dias and Basile 2013). The younger sediments on top of the Carboniferous Flysch of SW Portugal is at least Middle to Upper Triassic (Palain 1976), but possibly could attain the Lower Triassic (Rocha 1976). In Ponta Ruiva, the Triassic sediments have been shown to be syn-rift in relation to the early extensional stages of the Atlantic opening (Fig. 11B; Dias and Ribeiro 2002). As the D_1 age should be close to the local Carboniferous sedimentation (i.e. Upper Moscovian) and the D_2 shear zones have been reactivated as normal faults during the Triassic extension, the age of D_2 phase is bracketed by these two events. This means that the D_2 in SW Portuguese coast must be considered a Late Variscan tectonic event, acting during Late Carboniferous and Permian times, as emphasized

by Noronha et al. (1981) for the Central Iberian Zone in Northern Portugal.

The NNE–SSW Late Variscan kinematics

As the Almograve structural data show (Fig. 9C), the NNE–SSW faults have a sinistral kinematics. This behaviour is pervasive along the SW Portuguese coast, where NNE–SSW to NE–SW hectometric faults and/or kink bands with metric to decametric sinistral displacements are common (Caroça and Dias 2002; Dias and Basile 2013). The strongly linear NNE–SSW trend of this coast seems to indicate that it is controlled by a deep first-order Late Variscan sinistral fault, whose superficial expression is the second- and third-order sinistral fault like structures found in Almograve-type faults (Fig. 15A; Caroça and Dias 2002; Dias and Basile 2013). The obliquity between both scales of faults indicates that the minor ones could be interpreted as p-type fractures inside a main shear zone (Fig. 15A). A comparison of the trend of the D_2 sinistral fractures of Almograve (NNE–SSW; Fig. 3) with those observed further to SW (NE–SW; Caroça and Dias 2002) shows a slight rotation (Fig. 15A_1, A_2). Such rotation accompanies the linear orientation of the Portuguese coast.

The existence of a probable major NNE–SSW Late Variscan left-lateral fault in SW Iberia shows that the dominant trend of Late Variscan faults in northern Portugal (e.g. Vilariça and Régua-Chaves-Verin first-order faults; Fig. 15B) is also found further south (Fig. 15A). As in SW Portugal the sinistral kinematics is clear (Figs. 4, 9C), the same kinematics must be expected in the Northern Portugal NNE–SSW faults. Nevertheless, although the sinistral kinematics during Late Variscan times is usually considered (Ribeiro 1974; Ribeiro et al. 1979; Iglesias and Ribeiro 1981; Choukhroune and Iglésias 1980; Pereira et al. 1993; Ribeiro et al. 2007; Moreira et al. 2010, 2014; Dias et al. 2013), an alternative proposal is that the sinistral sense was only an alpine reworking of a dextral NNE–SSW Late Variscan kinematics (Marques et al. 2002; Lourenço et al. 2002).

The dextral interpretation was based essentially in the K–Ar 312 Ma age in muscovites concentrates from aplites and tourmaline–muscovite aggregates related to NE–SW segments in NNE–SSW faults in Northern Portugal (Marques et al. 2002) and the geometrical/kinematical data from quartz veins, which are difficult to ascribe to the different tectonic events. Although these authors considered the obtained age a lower limit for the Late Variscan wrench faulting period, it could also be considered the upper limit for the D_3 Variscan regional event (Dallmeyer et al. 1997). Thus, the proposed dextral movement along the NNE–SSW fault set should be considered as related, not with the Late Variscan kinematics (Marques et al. 2002), but with the

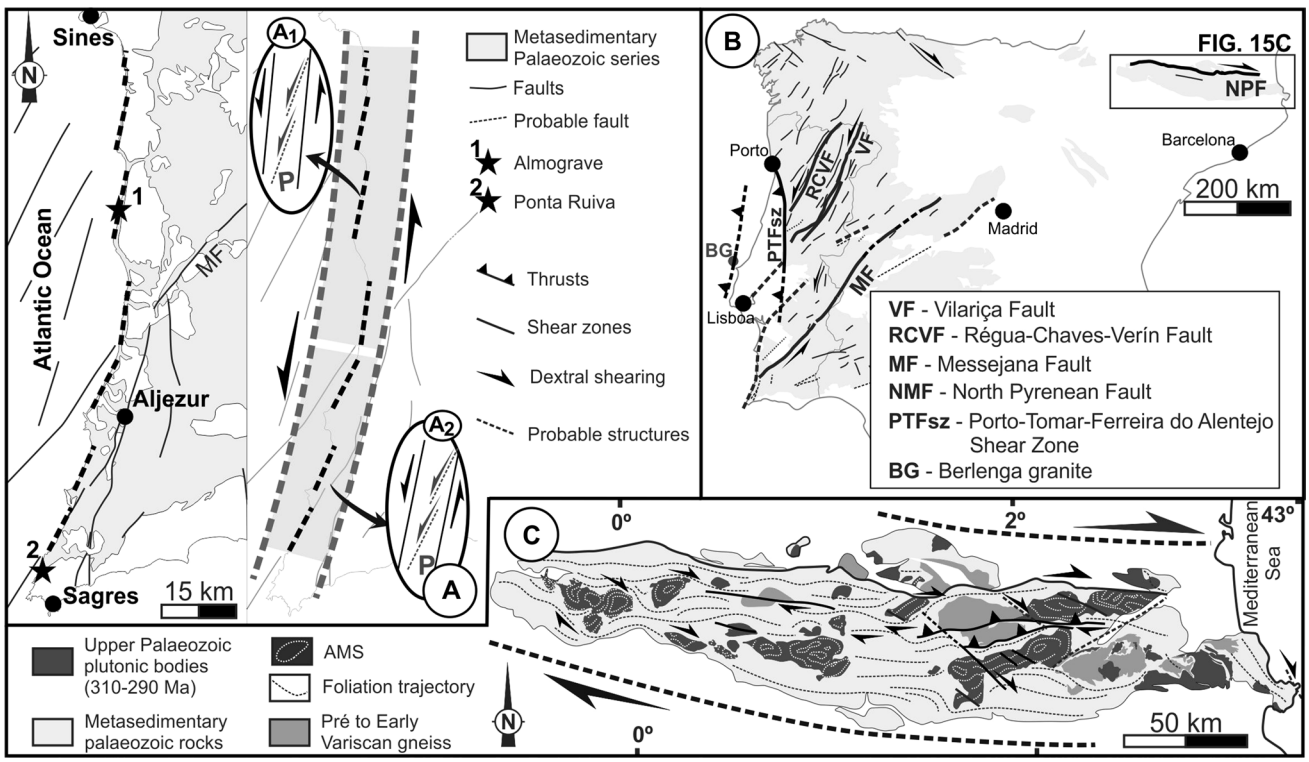

Fig. 15 Late Variscan structural behaviour in Iberia. **A** Interpretative fracture pattern along the SW Portuguese coast; **B** main fracture pattern in Iberia; **C** structural sketch of the Variscan Pyrenees (adapted from Zwart 1986; Carreras 2001; Denèle et al. 2014)

regional D_3 Variscan tectonic event as previously reported in several works (Ribeiro 1974; Ribeiro et al. 1979; Pereira et al. 1993; Dias et al. 2013; Noronha et al. 2013). Therefore, the new data in SW Portuguese coast show that the predominant movement in the NNE–SSW to NE–SW faults during Late Variscan times (i.e. Post-Moscovian–Pre-Triassic) was left-lateral, as proposed in early works (Ribeiro 1974; Arthaud and Matte 1975, 1977; Ribeiro et al. 1979; Choukhroune and Iglésias 1980; Iglesias and Ribeiro 1981).

The E–W to ENE–WSW dextral kinematics

Even if the NNE–SSW fracture pattern has a pervasive development in Iberia (Fig. 15B), the SW Portuguese data show that the Late Variscan deformation cannot be understood without taking into account the E–W to ENE–WSW dextral shear zones. Indeed, although the sinistral NNE–SSW trend is usually more common, the dextral one sometimes becomes predominant.

The E–W to ESE–WNW structural trend is dominant in the axial zone of Pyrenees, in the Neoproterozoic and Palaeozoic rocks (Fig. 15C; e.g. Zwart 1986; Castiñeiras et al. 2008), where a polyphasic tectonothermal evolution with three Variscan deformation events is found (Carreras 2001; Druguet 2001). Such trend is usually correlated with the main Variscan tectonometamorphic event (local D_2) characterized by a dextral transpressional regime (Carreras and Druguet 1994; Leblanc et al. 1996; Druguet and Hutton 1998; Gleizes et al. 1998; Carreras 2001; Druguet 2001; Carreras et al. 2004; Druguet et al. 2014). The D_2 event is related to a progressive high-temperature low-pressure metamorphic event (Druguet and Hutton 1998; Druguet 2001; Druguet et al. 2014) associated with melt generation and the emplacement of an important set of plutonic bodies. Recent geochronological data constrain the age of emplacement of these syntectonic bodies between 310 and 290 Ma (i.e. Carboniferous–Permian transition; Denèle et al. 2014; Druguet et al. 2014; Pereira et al. 2014) and consequently also constrain the age of the D_2 event. The anisotropy of magnetic susceptibility (AMS) shows clear evidence of dextral kinematics during the emplacement of these D_2 syntectonic plutonic bodies (Fig. 15C; Leblanc et al. 1996; Gleizes et al. 1997, 1998; Antolín-Tomás et al. 2009; Denèle et al. 2014). Gleizes et al. (1997, 1998) also remark the presence of continuous deformation from the magmatic state to the high-temperature solid state, which shows that dextral transpression remained active even after the emplacement. The previous data highlight an important Late Variscan WNW–ESE dextral transpressive shear zone in the basement of the Axial Zone of the Pyrenees, which remained active from the Late Carboniferous until at least the Lower Permian.

Further South in Iberia, the predominance of E–W major right-lateral shear zones during Late Variscan times could also be emphasized in the Azores–Gibraltar shear zone (Fig. 16; Ribeiro et al. 2007; Dias et al. 2016). However, these kinematics are poorly constrained due to their reworking as a plate boundary during the Pangaea breakup and the Alpine orogeny.

The major role that the E–W shear zones play in Iberia could be extended to the neighbouring regions. Indeed, they are also found, not only in Southern France

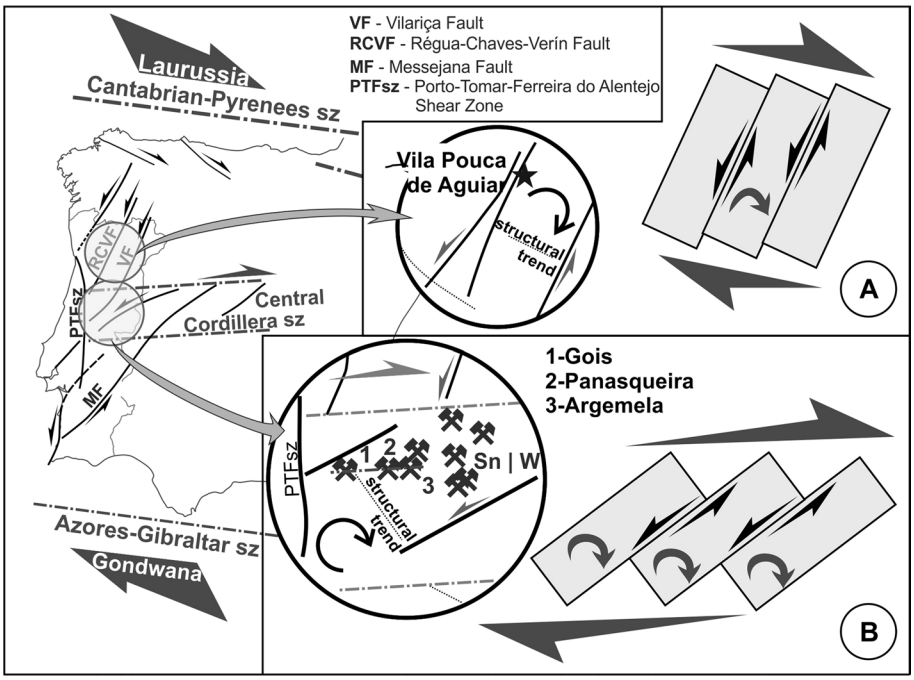

Fig. 16 Interpretative domino model for Iberian geodynamics during Late Variscan times (adapted from Ribeiro 2002; ore occurrences adapted from Pereira et al. 1993 and Noronha et al. 2013). **A** NNE–SSW faults related to a low block rotation; **B** NE–SW faults related to a moderate/strong block rotation

(Martínez-García 1996), but also in the Moroccan Variscides (Piqué et al. 1990; Houari and Hoepffner 2003; Simancas et al. 2005; Ribeiro et al. 2007). Although such major shear zones were already active since the main orogenic events, sometimes they are considered to be still active in Late Variscan times (Ribeiro et al. 2007; Dias et al. 2011).

An unifying approach

The absence of the dextral conjugated set (which in a brittle to brittle–ductile regime should be NNW–SSE; Ribeiro et al. 1979), the relatively moderate offset comparing to the extension of the NNE–SSW major faults and the existence of N–S Late Variscan thrusts with an eastern displacement in the Berlengas Archipelago (Fig. 15B) led Ribeiro (2002) to proposing a domino model for the Late Variscan deformation (Fig. 16).

In this model, the dextral transpression induced by the Late Variscan oblique collision between Laurentia and Gondwana (Arthaud and Matte 1975, 1977; Dias and Ribeiro 1994, 1995; Ribeiro et al. 1995; Shelley and Bossière 2000, 2002; Ribeiro 2002; Ribeiro et al. 2007; Dias et al. 2016) was mostly concentrated in the major E–W Iberian shear zones, located in Azores–Gibraltar and North Pyrenean shear zones. The domains between these shear zones were heterogeneously deformed. The important regional D_3 NNE–SSW tensile fractures in Central Iberian Zone (Ribeiro 1974; Pereira et al. 1993; Mateus 1995) were rotated clockwise during the Late Variscan times. Such movement gave rise to a dextral domino due to the clockwise rotation of the blocks bounded by the NNE–SSW faults, which thus will have a coeval sinistral kinematics (Fig. 16A, B; Ribeiro 2002; Ribeiro et al. 2007).

As expected, in a domino model, the amount of block rotation is strongly related to the intensity of distortion induced by the simple shear component. In Iberia, this is supported by the trend of the major sinistral Late Variscan faults (Dias et al. 2013). The rotation from a NNE–SSW trend, either in northern (Fig. 16A; Régua-Chaves-Verin and Vilariça faults), or southern (Fig. 16; Messejana fault) sectors, to a NE–SW on Central Iberia (Fig. 16B), is explained by the lesser or stronger influence of the major ENE–WSW dextral Central Cordillera shear zone (Ribeiro 2002). The same rotation is also observed using the main regional D_1 Variscan structures, whose general trend of folds has a WNW–ESE direction in Northern Portugal (Fig. 16A), and a NW–SE in Central Portugal (Fig. 16B). The Central Cordillera shear zone is also enhanced by discrete E–W Late Variscan lineaments of Late Variscan mineralizations like the tin–tungsten–gold Góis–Panasqueira–Argemela band (Fig. 16B; Ribeiro and Pereira 1982).

A similar deflection is found in the SW Portuguese coast (Caroça and Dias 2002), with the main Late Variscan fractures rotating from NNE–SSW (Fig. $15A_1$) towards NE–SW in the southern sectors (Fig. 15B). Such behaviour should be expected due to a closer proximity of the first-order E–W dextral Azores–Gibraltar shear zone.

Conclusions

The principal outcomes of this study are concluded below:

1. The Variscan structures in the SW of South Portuguese Zone are the result of a long-lasting diachronic process during the D_1 tectonic event, followed by D_2 deformation ascribed to the Late Variscan times;
2. The NNE–SSW Late Variscan faults have a predominantly sinistral kinematics;
3. The Late Variscan fault pattern in Iberia could be explained by a domino model controlled by E–W to ENE–WSW major dextral strike-slip shear zones, inducing the clockwise rotation of the blocks bounded by the NNE–SSW faults;
4. This model could be considered an improvement in the dextral E–W mega-shear model of Arthaud and Matte (1975, 1977), between what they considered a northern American–European plate and a southern African one.

Acknowledgements We are grateful to Prof. Paul Ryan and an anonymous referee for their insightful reviews and many constructive suggestions for improvement in the manuscript. The careful editorial work of Martínez Catalán also helps to clarify several parts of the text. The authors also acknowledge the funding provided by the Institute of Earth Sciences (ICT), under contract with FCT (the Portuguese Science and Technology Foundation; UID/GEO/04683/2013). Noel Moreira acknowledges Fundação Calouste Gulbenkian for the financial support and the FCT Ph.D. Grant (SFRH/BD/80580/2011). António Ribeiro acknowledges the financial support by FCT Project UID/GEO/50019/2013—Instituto Dom Luiz.

References

Abad I, Nieto F, Vellila N, Simancas J (2004) Metamorfismo de la Zona Sudportuguesa. In: Vera JA (ed) Geologia de Espana. SGE-IGME, Madrid, pp 209–211

Antolín-Tomás B, Román-Berdiel T, Casas-Sainz A, Gil-Peña I, Oliva B, Soto R (2009) Structural and magnetic fabric study of the Marimanha granite (Axial Zone of the Pyrenees). Int J Earth Sci (Geol Rundsch) 98:427–441. doi:10.1007/s00531-007-0248-1

Arthaud F, Matte Ph (1975) Les decrochements tardi-hercyniens du sud-ouest de l'Europe, geometrie et essai de reconstitution des conditions de la deformation. Tectonophysics 25:139–171. doi:10.1016/0040-1951(75)90014-1

Arthaud F, Matte Ph (1977) Late Paleozoic strike-slip faulting in southern Europe and northern Africa: result of a righ-lateral shear zone between the Appalachians and the Urals. Geol Soc Am Bull 88:1305–1320. doi:10.1130/0016-7606(1977)88<1305:LPSFIS>2.0.CO

Belayneh M, Cosgrove J (2010) Hybrid veins from the southern margin of the Bristol Channel Basin, UK. J Struct Geol 32:192–201. doi:10.1016/j.jsg.2009.11.010

Bradley DC, Kidd WSF (1991) Flexural extension of the upper continental crust in collisional foredeeps. Geol Soc Am Bull 103(11):1416–1438. doi:10.1130/0016-7606(1991)103<1416:FEOTUC>2.3.CO;2

Caroça C, Dias R (2001) Estrutura Varisca na região de Sagres; um exemplo de deformação progressiva. Comun Inst Geol Min Port 88:1–16

Caroça C, Dias R (2002) Deformação transcorrente nos sectores externos da zona Sul Portuguesa; os últimos incrementos da tectónica Varisca. Comun Inst Geol Min Port 89:115–126

Carreras J (2001) Zooming on Northern Cap the Creus shear zones. J Struct Geol 23:1457–1486. doi:10.1016/S0191-8141(01)00011-6

Carreras J, Druguet E (1994) Structural zonation as a result of inhomogeneous non-coaxial deformation and its control on syntectonic intrusions: an example from the Cap de Creus area (eastern-Pyrenees). J Struct Geol 16:1525–1534. doi:10.1016/0191-8141(94)90030-2

Carreras J, Druguet E, Griera A, Soldevila J (2004) Strain and deformation history in a syntectonic pluton. The case of the Roses granodiorite (Cap de Creus, Eastern Pyrenees). Geological Society, London, Special Publications 224, pp 307–319. doi:10.1144/GSL.SP.2004.224.01.19

Carvalho D, Goinhas J, Oliveira V, Ribeiro A (1971) Observações sobre a geologia do Sul de Portugal e consequências metalogenéticas. Est Notas e Trab Serv Fom Min 20:153–199

Castiñeiras P, Navidad M, Liesa M, Carreras J, Casas JM (2008) U-Pb zircon ages (SHRIMP) for Cadomian and Early Ordovician magmatism in the Eastern Pyrenees: new insights into the pre-Variscan evolution of the northern Gondwana margin. Tectonophysics 461:228–239. doi:10.1016/j.tecto.2008.04.005

Choukhroune P, Iglésias M (1980) Zonas de cisalla dúctil en el NW de la Peninsula Ibérica. Cuad Lab Xeol Laxe 1:163–164

Coke C, Dias R, Ribeiro A (2003) Rheologically induced structural anomalies in transpressive regimes. J Struct Geol 25(3):409–420. doi:10.1016/S0191-8141(02)00043-3

Cosgrove J (1997) Hydraulic fractures and their implications regarding the state of stress in a sedimentary sequence during burial. In: Sengupta S (ed) Evolution of geological structures in micro- to macro-scales. Chapman & Hall, London, pp 11–25. doi:10.1007/978-94-011-5870-1_2

Cosgrove J (2005) Tectonics: fractures (including joints). In: Selley RC, Cocks LRM, Plimer IR (eds) Encyclopedia of geology. Elsevier, Amsterdam, pp 352–361

Dallmeyer D, Martínez Catalán J, Arenas R, Gil Ibarguchi J, Gutiérrez Alonzo G, Farias P, Bastida F, Aller J (1997) Diachronous Variscan tectonothermal activity in the NW Iberian Massif: evidence from 40Ar/39Ar dating of regional fabrics. Tectonophysics 277:307–337. doi:10.1016/S0040-1951(97)00035-8

Denèle Y, Laumonier B, Paquette J, Olivier P, Gleizes G, Barbey P (2014) Timing of granite emplacement, crustal flow and gneiss dome formation in the Variscan segment of the Pyrenees. Geological Society, London, Special Publications 405, pp 265–287. doi:10.1144/SP405.5

Dias R, Basile C (2013) Estrutura dos sectores externos da Zona Sul Portuguesa; implicações geodinâmicas. In: Dias R, Araújo A, Terrinha P, Kullberg JC (eds) Geologia de Portugal, vol 1. Escolar Editora, Lisbon, pp 787–807

Dias R, Ribeiro A (1994) Constriction in a transpressive regime: an example in the Ibero-Armoricain Arc. J Struct Geol 16(11):1543–1554. doi:10.1016/0191-8141(94)90032-9

Dias R, Ribeiro A (1995) The Ibero-Armorican arc: a collisional effect against an irregular continent? Tectonophysics 246(1–3):113–128. doi:10.1016/0040-1951(94)00253-6

Dias R, Ribeiro C (2002) O Triásico da Ponta Ruiva (Sagres); um fenómeno localizado na Bacia Mesozóica Algarvia. Comun Inst Geol Min Port 89:39–46

Dias R, Hadani M, Leal Machado I, Adnane N, Hendaq Y, Madih K, Matos C (2011) Variscan structural evolution of the western High Atlas and the Haouz plain (Morocco). J Afr Earth Sci 61:331–342. doi:10.1016/j.jafrearsci.2011.07.002

Dias R, Ribeiro A, Coke C, Pereira E, Rodrigues J, Castro P, Moreira N, Rebelo J (2013) Evolução estrutural dos sectores setentrionais do autóctone da Zona Centro-Ibérica. In: Dias R, Araújo A, Terrinha P, Kullberg JC (eds) Geologia de Portugal, vol 1. Escolar Editora, Lisbon, pp 73–147

Dias R, Ribeiro A, Romão J, Coke C, Moreira N (2016) A review of the arcuate structures in the Iberian Variscides; constraints and genetical models. Tectonophysics 681:170–194. doi:10.1016/j.tecto.2016.04.011

Druguet E (2001) Development of high thermal gradients by coeval transpression and magmatism during the Variscan orogeny: insights from the Cap de Creus (Eastern Pyrenees). Tectonophysics 332:275–293. doi:10.1016/S0040-1951(00)00261-4

Druguet E, Hutton D (1998) Syntectonic anatexis and magmatism in a mid-crustal transpressional shear zone: an example from the Hercynian rocks of the eastern Pyrenees. J Struct Geol 20:905–916. doi:10.1016/S0191-8141(98)00017-0

Druguet E, Castro A, Chichorro M, Pereira M, Fernández C (2014) Zircon geochronology of intrusive rocks from Cap de Creus, Eastern Pyrenees. Geol Mag 151(6):1095–1114. doi:10.1017/S0016756814000041

Gleizes G, Leblanc D, Bouchez J (1997) Variscan granites of the Pyrenees revisited: their role as syntectonic markers of the orogen. Terra Nova 9:38–41. doi:10.1046/j.1365-3121.1997.d01-9.x

Gleizes G, Leblanc D, Santana V, Olivier Ph, Bouchez J (1998) Sigmoidal structures featuring dextral shear during emplacement of the Hercynian granite complex of Cauterets–Panticosa (Pyrenees). J Struct Geol 20(9–10):1229–1245. doi:10.1016/S0191-8141(98)00060-1

Houari M, Hoepffner C (2003) Late Carboniferous dextral wrench-dominated transpression along the North African craton margin (Eastern High-Atlas, Morocco). J Afr Earth Sci 37:11–24. doi:10.1016/S0899-5362(03)00085-X

Iglesias M, Ribeiro A (1981) Zones de cisaillement ductile dans l'arc ibéro-armoricain. Comun Serv Geol Port 67:85–87

Jorge R, Fernandes P, Rodrigues B, Pereira Z, Oliveira JT (2013) Geochemistry and provenance of the Carboniferous Baixo Alentejo Flysch Group, South Portuguese Zone. Sed Geol 284(285):133–148. doi:10.1016/j.sedgeo.2012.12.005

Leblanc D, Gleizes G, Roux L, Bouchez J (1996) Variscan dextral transpression in the French Pyrenees: new data from the Pic des Trois-Seigneurs granodiorite and its country rocks. Tectonophysics 261:331–345. doi:10.1016/0040-1951(95)00174-3

Lourenço J, Mateus A, Coke C, Ribeiro A (2002) A zona de falha Penacova-Régua-Verín na região de Telões (Vila Pouca de Aguiar); alguns elementos determinantes da sua evolução em tempos tardivariscos. Comun Inst Geol Min 89:105–122

Marques F, Mateus A, Tassinari C (2002) The Late-Variscan fault network in central-northern Portugal (NW Iberia): a re-evaluation. Tectonophysics 359:255–270. doi:10.1016/S0040-1951(02)00514-0

Marques F, Burg J, Lechmann S, Schmalholz S (2010) Fluid-assisted particulate flow of turbidites at very low temperature: a key to tight folding in a submarine Variscan foreland basin of SW Europe. Tectonics. doi:10.1029/2008TC002439

Martínez Catalán J (2011) Are the oroclines of the Variscan belt related to late Variscan strike-slip tectonics? Terra Nova 23:241–247

Martínez-García E (1996) Correlation of Hercynian units of the Iberin massif and southeartern France. Geogaceta 20(2):468–471

Mateus A (1995) Evolução tectono-térmica e potencial metalogenético do troço transmontano da Zona da Falha Manteigas-Vilariça-Bragança, Ph.D. Thesis, Lisbon University

Moreira N, Dias R, Coke C, Búrcio M (2010) Partição da deformação Varisca nos sectores de Peso da Régua e Vila Nova de Foz Côa

(Autóctone da Zona Centro Ibérica); Implicações Geodinâmicas. Comunicações Geológicas 97:147–162
Moreira N, Araújo A, Pedro JC, Dias R (2014) Geodynamic evolution of Ossa-Morena Zone in SW Iberian context during the Variscan Cycle. Comunicações Geológicas 101(I):275–278
Munhá J (1983) Hercynian magmatism in the Iberian Pyrite Belt. In: Lemos de Sousa M, Oliveira JT (eds) The Carboniferous of Portugal. Memórias dos Serviços Geológicos de Portugal 29, pp 39–81
Nance R, Gutiérrez-Alonso G, Keppie J, Linnemann U, Murphy J, Quesada C, Strachan R, Woodcock N (2012) A brief history of the Rheic Ocean. Geosci Front 3(2):125–135. doi:10.1016/j.gsf.2011.11.008
Noronha F, Ramos JMF, Rebelo JA, Ribeiro A, Ribeiro ML (1981) Essai de corrélation des phases de déformation hercynienne dans le nord-ouest Peninsulaire. Leidse Geol Meded 52(1):87–91
Noronha F, Ribeiro MA, Almeida A, Dória A, Guedes A, Lima A, Martins HC, Sant'Óvaia H, Nogueira P, Martins T, Ramos R, Vieira R (2013) Jazigos Filonianos Hidrotermais e Aplitopegmatíticos espacialmente associados a Granitos (Norte de Portugal). In: Dias R, Araújo A, Terrinha P, Kullberg JC (eds) Geologia de Portugal, vol 1. Escolar Editora, Lisbon, pp 403–438
Oliveira JT (1984) Carta geológica de Portugal. Escala 1/200.000. Notícia explicativa da Folha 7 (coord), Serviços Geológicos de Portugal
Oliveira JT (1990) South Portuguese Zone, stratigraphy and synsedimentary tectonism. In: Dallmeyer R, Martinez Garcia E (eds) Pre-mesozoic geology of Iberia. Springer, Berlin, pp 334–347
Oliveira JT, Relvas J, Pereira Z, Matos J, Rosa C, Rosa D, Munhá J, Fernandes P, Jorge RCGS, Pinto A (2013) Geologia da Zona Sul Portuguesa, com ênfase na estratigrafia, vulcanologia física, geoquímica e mineralizações da Faixa Piritosa. In: Dias R, Araújo A, Terrinha P, Kullberg JC (eds) Geologia de Portugal, vol 1. Escolar Editora, Lisbon, pp 673–765
Palain C (1976) Une série détritique terrigéne. Les Grés de Silves. Trias et Lias inférieur du Portugal, Mem. 25 (Nova Série) Serviços Geológicos de Portugal
Pereira E, Ribeiro A, Meireles C (1993) Cisalhamentos hercínicos e controlo das mineralizações de Sn-W, Au e U na Zona Centro-Ibérica em Portugal. Cuaderno Lab Xeolóxico de Laxe 18:89–119
Pereira Z, Matos J, Fernandes P, Oliveira JT (2007) Devonian and Carboniferous palynostratigraphy of the South Portuguese Zone, Portugal—an overview. Comunicações Geológicas 94:53–79
Pereira MF, Castro A, Chichorro M, Fernández C, Díaz-Alvarado J, Martí M, Rodríguez C (2014) Chronological link between deep-seated processes in magma chambers and eruptions: permo-Carboniferous magmatism in the core of Pangaea (Southern Pyrenees). Gondwana Res 25:290–308. doi:10.1016/j.gr.2013.03.009
Piqué A, Cornee J, Muller J, Roussel J (1990) The Moroccan Hercynides. In: Dallmeyer RD, Lécorché JP (eds) The West African orogens and circum Atlantic correlatives. Springer, Berlin, pp 229–262
Price N, Cosgrove J (1990) Analysis of geological structures. Cambridge University Press, Cambridge
Ramsay J, Huber M (1987) The techniques of modern structural geology. Volume 2: folds and fractures. Academic Press Inc, London
Reber J, Schmalholz S, Burg J (2010) Stress orientation and fracturing during three-dimensional buckling: numerical simulation and application to chocolate-tablet structures in folded turbidites, SW Portugal. Tectonophysics 493:187–195. doi:10.1016/j.tecto.2010.07.016
Ribeiro A (1974) Contribuition à l'étude tectonique de Trás-os-Montes. Mem Serv Geol Portugal, 24
Ribeiro A (1983) Structure of the Carrapateira nappe in Bordeira area south–west Portugal. In: Lemos de Sousa MJ, Oliveira JT (eds) The Carboniferous of Portugal, Mem. Serv. Geol. Portugal 29:91–97
Ribeiro A (2002) Soft plate tectonics. Springer, Berlin
Ribeiro A, Pereira E (1982) Controles paleogeográficos, petrológicos e estruturais na génese dos jazigos portugueses de estanho e volfrámio. Geonovas 1(3):23–31
Ribeiro A, Antunes M T, Ferreira MP, Rocha RB, Soares AF, Zbyszewski G, Moitinho de Almeida F, Carvalho D, Monteiro J H (1979) Introduction à la Géologie Générale du Portugal. Serviços Geológicos de Portugal
Ribeiro A, Oliveira JT, Silva J (1983) La estrutura de la Zona Sur Portuguesa. In: Comba JA (ed), Geologia de España, vol 1, Inst. Geol. Min. Esp. Madrid, pp 504–511
Ribeiro A, Pereira E, Dias R (1990) Structure of Centro-Iberian allochthon in northern Portugal. In: Dallmeyer R, Martinez Garcia E (eds) Pre-mesozoic geology of Iberia. Springer, Berlin, pp 220–236
Ribeiro A, Dias R, Silva J (1995) Genesis of the Ibero-Armorican Arc. Geodin Acta 8(2):173–184. doi:10.1080/09853111.1995.11417255
Ribeiro A, Munhá J, Dias R, Mateus A, Pereira E, Ribeiro L, Fonseca P, Araújo A, Oliveira T, Romão J, Chaminé H, Coke C, Pedro J (2007) Geodynamic evolution of SW Europe Variscides. Tectonics 26:1–24. doi:10.1029/2006TC002058
Rocha R (1976) Estudo estratigráfico e paleontológico do Jurássico do Algarve ocidental. Ciências Terra, 2
Schermerhorn L (1971) An outline stratigraphy of the Iberian Pyrite Belt. Bol Geol Min España 82(3–4):239–268
Scisciani V, Calamita F, Tavarnelli E, Rusciadelli G, Ori GG, Paltrinieri W (2001) Foreland-dipping normal faults in the inner edges of syn-orogenic basins: a case from the Central Apennines, Italy. Tectonophysics 330:211–224. doi:10.1016/S0040-1951(00)00229-8
Shelley D, Bossière G (2000) A new model for the Hercynian Orogen of Gondwanan France and Iberia. J Struct Geol 22:757–776. doi:10.1016/S0191-8141(00)00007-9
Shelley D, Bossière G (2002) Megadisplacements and the Hercynian orogen of Gondwanan France and Iberia. Geological Society of America Special Papers 364, pp 209–222. doi:10.1130/0-8137-2364-7.209
Silva J (1989) Estrutura de uma geotransversal da faixa piritosa: zona do vale do Guadiana. Ph.D. Thesis, Lisbon University
Silva J, Oliveira J, Ribeiro A (1990) South Portuguese Zone, structural outline. In: Dallmeyer R, Martinez Garcia E (eds) Pre-mesozoic geology of Iberia. Springer, Berlin, pp 348–362
Silva J, Pereira M, Chichorro M (2013) Estrutura das áreas internas da Zona Sul Portuguesa, no contextodo Orógeno Varisco. In: Dias R, Araújo A, Terrinha P, Kullberg JC (eds) Geologia de Portugal, vol 1. Escolar Editora, Lisbon, pp 767–786
Simancas J, Tahiri A, Azor A, Lodeiro F, Poyatos D, Hadi H (2005) The tectonic frame of the Variscan-Alleghanian orogen in southern Europe and Northern Africa. Tectonophysics 398:181–198. doi:10.1016/j.tecto.2005.02.006
Twiss R, Moores E (1992) Structural geology. W. H. Freeman and Company, San Francisco
Ribeiro A, Silva J (1983) Structure of the South Portuguese Zone. In: Lemos de Sousa MJ, Oliveira JT (eds) The Carboniferous of Portugal, Mem. Serv. Geol. Portugal 29:83–89
Zulauf G, Gutiérrez-Alonso G, Krausc R, Petschick R, Potel S (2011) Formation of chocolate-tablet boudins in a foreland fold and thrust belt: a case study from the external Variscides (Almograve, Portugal). J Struct Geol 33:1639–1649. doi:10.1016/j.jsg.2011.08.009
Zwart H (1986) The Variscan geology of Pyrenees. Tectonophyics 129:9–27. doi:10.1016/0040-1951(86)90243-X